



TAMPEREEN TEKNILLINEN YLIOPISTO
TAMPERE UNIVERSITY OF TECHNOLOGY

PAAVO JÄNTTI
SOLAR CELLS WITH METHYLAMMONIUM LEAD HALIDE
PEROVSKITES
Master of Science Thesis

Examiner: professor Helge Lem-
metyinen
Examiner and topic approved by the
faculty meeting of the faculty of nat-
ural sciences on 14th of January
2014

ABSTRACT

TAMPERE UNIVERSITY OF TECHNOLOGY

Master's Degree Programme in Science and Engineering

JÄNTTI, PAAVO: Solar cells with methylammonium lead halide perovskites

Master of Science Thesis, 59 pages, 35 Appendix pages

January 2015

Major: Chemistry

Examiner: Professor Helge Lemmetyinen, PhD Tero Kesti

Keywords: perovskites, organic-inorganic solar cells, methylammonium lead halides

Methylammonium lead halide perovskites are proving to be extremely efficient photo-active components of organic-inorganic solar cells. Though their suitability for photovoltaics was discovered only recently, the results acquired are improving more rapidly than with any other type of solar cell.

In this work perovskite cells were studied by making them in the laboratory by starting with the recipe from Shi et al. (2014a). The first cells were not very efficient, but alterations, to accommodate for the conditions, were made and the second set was significantly better. The recipe was further modified according to other published works and the 3rd and 4th sets were even better.

The cells made had a lot of variation and therefore it is hard to say, which improvements to the recipe actually caused the better performance. The improvements that were most likely to increase cell performance were the heating of the substrates before spin coating them with the lead halide solution and the introduction of lead chloride in small concentrations to the lead halide solution used for spin coating.

As the research went on, other directions apart from just tweaking the recipe came along and were duly studied with hopes of discovering something new. A perovskite powder was manufactured in a solution as well as via a solid-state reaction. The powder was then compressed into a pellet to study, if it was feasible to fabricate perovskite cells by this way as well. The resulting tablets were too brittle and hard to handle and due to lack of time this direction was abandoned.

Attempts were made to make perovskite films in dimethylformamide (DMF), by making a supersaturated solution of lead halides and methylammonium iodide (MAI), as the solution of both solutes is highly dependent on the temperature of the solution. However the attempts to achieve a supersaturated solution, in which, upon cooling, perovskite would form, proved futile. The solution made was used to make a set of cells with the one-step precursor deposition.

When testing the solubility of different lead halides it was discovered that lead chloride is more soluble in cold DMF than hot. Another interesting fact is that the presence of MAI assists the solution of both lead halides significantly. They must form some kind of complexes with each other and DMF. MAI also undergoes a slow reaction to complexes in 2-propanol, as observed by the changing of its colour in 2-propanol.

TIIVISTELMÄ

TAMPEREEN TEKNILLINEN YLIOPISTO

Teknisluonnontieteellinen koulutusohjelma

JÄNTTI, PAAVO: Solar cells with methylammonium lead halide perovskites

Diplomityö, 59 sivua, 35 liitesivua

Tammikuu 2015

Pääaine: Kemia

Tarkastaja: professori Helge Lemmetyinen, tohtori Tero Kesti

Avainsanat: perovskiitti, orgaaninen-epäorgaaninen aurinkokenno, metyyliammoniumlyijyhalidit

Metyyliammoniumlyijyhalidiperovskiitit vaikuttavat olevan erittäin tehokkaita orgaanis-epäorgaanisten aurinkokennojen komponentteja. Vaikka tämä soveltuvuus löydettiin vasta hiljattain, niiden avulla saadut tulokset paranevat nopeammin kuin minkään muun aurinkokennotyyppin.

Perovskiittirakenteisia kennoja tutkittiin tekemällä niitä laboratoriossa. Työn pohjareseptiksi valittiin Shi'n et al. (2014a) julkaisussa käytetty resepti. Ensimmäiset kennot eivät olleet kovin tehokkaita, mutta, kun reseptiä muunneltiin, toinen erä oli jo paljon parempi. Reseptiä kehiteltiin edelleen kirjallisuudesta saadun tiedon mukaisesti ja kolmas ja neljäs erä onnistuivat vielä paremmin.

Kennojen laatu vaihteli paljon, joten on vaikea sanoa, mitkä reseptin parannuksista johtivat parempaan suorituskykyyn. Substraattien lämmitys ennen spin-päällystämistä sekä pienen lyijykloridimäärän käyttö lyijyjodidiin seostettuna olivat todennäköisimmin onnistuneita parannuksia.

Tutkimuksen edetessä alettiin tutkia reseptin parantelun lisäksi muitakin kennojen toimintaan vaikuttavia tekijöitä. Perovskiittijauhetta valmistettiin kahdella tavalla, sekä liuoksessa että kiinteän olomuodon reaktiona. Jauheet puristettiin tablettiksi, jotta voitaisiin tutkia, syntyisikö toimivia perovskiittikennoja myös näin. Tabletit olivat kuitenkin liian hauraita ja vaikeita käsitellä ja projektin päättymisen vuoksi tätä ei tutkittu enempää.

Perovskiittikalvoja yritettiin valmistaa dimetyyliformaidi (DMF)-liuoksessa valmistamalla kyllästetyt liuokset lyijyhalideista ja metyyliammoniumjodidista (MAI). Tämän piti olla mahdollista sillä molempien liukoisuudet riippuvat voimakkaasti lämpötilasta. Ylikylläistä liuosta ei kuitenkaan saatu valmistettua ja valmistettuihin liuoksiin ei jäähtyessä muodostunut minkäänlaista sakkaa. Liuoksia käytettiin kuitenkin tekemään erä aurinkokennoja yhden askeleen menetelmällä.

Testattaessa lyijyhalidin liukoisuutta, havaittiin, että lyijykloridi liukenee paremmin kylmään kuin kuumaan DMF:ään. Mielenkiintoista oli myös, että MAI edesauttaa molempien lyijyhalidien liukenemistä merkittävästi. Havaittiin, että MAI vaihtaa hitaasti väriään 2-propanolissa. Tämä johtunee siitä, että MAI:ssa tapahtuu hidas kompleksireaktio 2-propanolissa.

PREFACE

This work was done under the supervision of PhD Tero Kesti. Tero advised me in planning of the experiments and provided valuable insight and literary material to help me better understand the phenomena I was working with. Without his contribution the making of this thesis would have been a lot more difficult and the result would have been undoubtedly different. So to him go my thanks.

I also wish to thank Professor Helge Lemmetyinen for giving me this opportunity to work with this project and topic, which is part of the work of the Supramolecular Photochemistry Group. Thanks are also due for his examination of my Thesis. The deadlines he set also helped me finish my Thesis in a much shorter time window than I believed possible.

I want to say thank you to my co-workers in the Chemistry lab for providing new ideas and spirited conversations both on and off topic. The atmosphere and feel of the working place created by the people working there helped me get the job done.

Thanks too to my girlfriend for listening to my occasional frustration and for making me work at home as well.

In Tampere, Finland, on the 12th of February 2015

Paavo Jäntti

Table of Contents

Abstract	ii
Terms and Definitions	vii
1 Introduction	9
2 Theoretical Background	11
2.1 Working principles of organic solar cells	11
2.1.1 Different types of organic solar cells	13
2.1.2 Characterization of the cells	16
2.2 History of perovskite	19
2.3 Preparation methods of perovskite solar cells	19
2.3.1 One-step precursor deposition	21
2.3.2 Sequential deposition method	21
2.3.3 Dual-source vapour deposition	21
2.3.4 Vapour assisted solution process	22
2.4 Perovskite properties	22
2.4.1 Crystal structure	22
2.4.2 Energy level	24
2.4.3 Charge carrier properties	24
3 Experimental	26
3.1 Cutting glass	26
3.2 Lead Iodide films on glass substrates	26
3.3 First set of solar cells	29
3.4 Measuring I-V curves	30
3.5 Refining the process of making a uniform layer of perovskite	31
3.6 Second set of solar cells	32
3.7 Monitoring the decay of the solar cells and further experiments with the solar simulator	32
3.8 Durability test	32
3.9 Perovskite tablets by pressing from powder	33
3.10 Single solution with lead iodide	34
3.11 Suspension in 2-propanol	35
3.12 Mixed halides	35
3.13 A set of mixed halide solar cells with 95:5 ratio of PbI₂ to PbCl₂	38
4 Results	41
4.1 Lead Iodide films on glass substrates	41
4.2 First solar cells with the recipe from Shi et al.	41
4.3 Refining the process of making a uniform layer of perovskite	43
4.4 Second set of solar cells	45
4.5 Monitoring the decay of the solar cells and further experiments with the solar simulator	47
4.6 Durability test	48
4.7 Perovskite pellets by pressing from powder	49

4.8	Single solution with lead iodide.....	51
4.9	Suspension in 2-propanol.....	53
4.10	Mixed halides.....	53
4.11	A set of mixed halide solar cells with 95:5 ratio of PbI₂ to PbCl₂	54
5	Conclusions.....	55
	References.....	57

TERMS AND DEFINITIONS

Acceptor	The material closest to the anode. It is capable of accepting electrons. Electrons travel well in this material and it is also known as electron transfer material (ETM) or layer (ETL).
DMF	N,N-dimethylformamide is the solvent used for dissolving lead halides in most of the experiments in this work.
Donor	The material closest to the cathode. It is capable of donating electrons. Holes travel well in this material and it is also known as hole transfer material (HTM) or layer (HTL)
Exciton	An excited state that forms and travels in an organic photo-active material. It splits into charge carries once it meets a boundary in the photoactive material or if the exciton binding energy versus thermal energy is low enough also in the bulk of the material. Exciton lifetime and diffusion length are important factors in determining the limiting attributes of organic solar cells.
Fill Factor, FF	The ratio of maximum power point to the theoretical maximum power of the cell if open-circuit voltage and short-circuit current had their highest values in the same point.
I-V curve	I-V curve presents the current (I) as the function of the voltage (V) in measurements made to determine the efficiency of an organic solar cell. In this measurement current is being measured while bias voltage to the cell is increased or decreased gradually.
Lead Halide	PbI_2 , PbBr_2 , PbCl_2
Maximum Power Point, P_{max}	P_{max} is the point on the I-V curve, where the absolute value of the product of current and voltage is the highest.
Open-Circuit Voltage, V_{oc}	V_{oc} is the maximum voltage that a cell can produce. In an I-V measurement this voltage is observed when $I = 0$. This voltage can be measured from an illuminated cell.
PCE	Power Conversion Efficiency is the ratio of output energy to input energy. It can be determined by measuring the I-V curve and comparing the acquired characteristics to the energy of intrinsic light.

Perovskite	A common name for a large group of materials with the same crystal structure, ABX_3 .
Short-Circuit Current, I_{sc}	I_{sc} is the maximum current that a cell can produce. In an I-V measurement this current is observed when $V=0$.
Spin coating	A method used to create thin films. A substrate is placed on a holder and the substance of which the film is to be made is dropped on the substrate and the substrate is then spun with an appropriate speed for an appropriate time.

1 INTRODUCTION

The fossil fuels that are used to create the bulk of the energy used by man are running out. Therefore new sources of energy must be found, if we are to continue to maintain and improve the standard of living acquired so far. Solar energy is an obvious choice for alternative energy as ultimately almost all energy forms used today are derived from ancient or not so ancient solar energy. All living things, apart from deep-dwelling bacteria using chemosynthesis (Aarhus University 2013), get their energy from the sun or from other organisms that do so. Why not make more direct use of the Sun's rays and use them to make electricity directly instead of first using it to grow crops and then burn that crop to power large water heaters.

Solar cells are one of the most feasible alternatives for fossil fuels and in some places the price of solar power competes well with the price of power from fossil fuels. With sufficient investment even with current technologies the power needed by the western countries could be provided almost solely by solar cells. In addition many different kinds of solar cells are being studied all the time. The various different approaches ensure breakthroughs and even better performing cells. (Snaith 2013)

Methylammonium lead halide perovskites are one of the most rapidly improving fields in solar cell technologies. These cells have only been studied for a few years and already their power conversion efficiencies approach 20 % (Green et al. 2015). The working principles of the cells are not yet fully understood and as we gain a more thorough understanding of these types of cells the efficiencies are bound to climb as well. The cells are relatively cheap, especially the photoactive material. They are also easy to manufacture in the laboratory scale, but not necessarily so in the industrial scale. This problem can surely be overcome with engineering directed at commercial manufacture. (Service 2013)

The perovskite cells are not without flaws however. A key component of the photoactive material is lead, which is poisonous and an environmental hazard. Experiments have been made with tin replacing the lead, but the resulting cells have had poorer performance achieving power conversion efficiencies of slightly above 6 %. (Noel et al. 2014) The efficiencies seem to deteriorate when exposed to sunlight for extended periods of time. The cells need to be well protected or they tend to lose all their activity and this makes the cells more complicated and therefore more expensive to manufacture. The cells should be stable for at least a few years for their use to be feasible otherwise the installation and replacement work is just too bothersome for the cells to be of real use. There are also many variables in making the cells that are not completely understood yet and sometimes the efficiencies acquired appear random. (Green et al. 2014)

These variables however provide a clear direction for new studies of the cells. When enough parameters have been studied thoroughly enough the cell performance will undoubtedly stabilize. This will result in well understood easy to manufacture high performance and affordable solar cells.

The aim of this thesis was to learn to understand how perovskite solar cells work, to make them and possibly discover something new. These kinds of cells were new to the research group, so there were not many practices to build on, except on the instruments. About the use of instruments the help from colleagues and clear written instructions were irreplaceable. Everything about the cells had to be learned from publications and by trial and error.

2 THEORETICAL BACKGROUND

This section presents some of the theory behind perovskite inorganic-organic solar cells starting from how solar cells work. There is a difference in how organic and inorganic solar cells work. The perovskite cells studied in this work while being organic-inorganic in other respects work more like the organic heterojunction solar cell portrayed in Figure 2.1.

2.1 Working principles of organic solar cells

In solar cells intrinsic light excites the photoactive material producing charge carriers. In conventional solar cells these are directly electrons and electron holes, while in organic solar cells an exciton is formed first. The exciton is not truly a particle like an electron is, but an excited state in one or several of the molecules of the photoactive material. The excited state “travels” from molecule to molecule until it meets a boundary in the material. At such a boundary the exciton may split into an electron and an electron hole. In conventional solar cells the anode is not transparent and light enters the cell next to the anode while in organic solar cells the cathode and anode are reversed and the cathode is transparent. This, along with the rest of the structure of conventional and organic solar cells, is shown in Figure 2.1. (Kumar & Chand 2012)

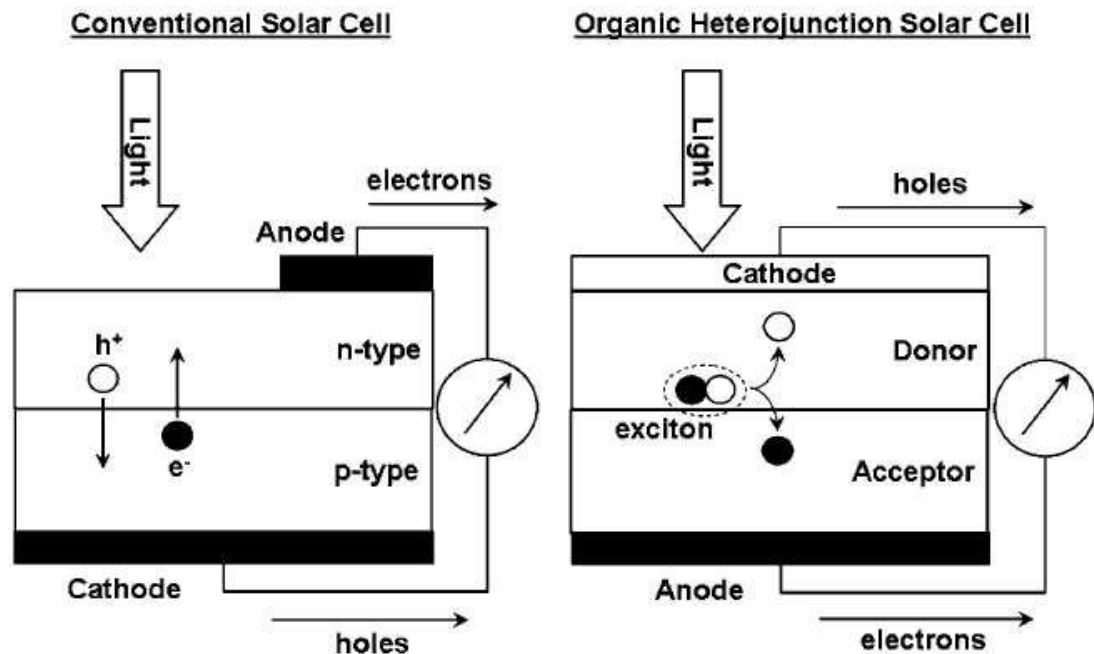


Figure 2.1. The structures of a conventional and an organic solar cell. (Benanti & Venkataraman 2006)

The simplest organic solar cell would have a transparent cathode, a light absorbing material and an anode. These cells aren't very effective though and a lot of improvements have been made to this architecture. An efficient modern solar cell could for instance consist of a substrate, a transparent cathode, an HTL, a scaffolding layer, a light absorbing layer, an ETL and an anode. (Kumar & Chand 2012)

The photoactive material in a cell absorbs a photon and is activated. This results in an excited state, an exciton. The electrons are excited to the lowest unoccupied molecular orbital (LUMO) leaving behind positive holes in the highest unoccupied molecular orbital (HOMO). This exciton can be handled like one would an electron-electron-hole-pair in a conventional semiconductor. The exciton travels in the photoactive material until it dissipates or reaches a boundary, where it breaks into an electron and a hole. The break is made possible by the difference in the work functions of the cathode, high work function, and the anode, low work function. Electrons travel to the anode and holes to the cathode generating a current and a potential difference, which can be harnessed into electricity. The cathode is often, like in this work, indium tin oxide and the anode is a metal like silver or gold. However in semiconductors, like perovskite, there is not a single molecule with its HOMOs and LUMOs instead there is a crystal lattice. In this lattice the molecular orbitals have merged into bands, namely the valence and the conduction band. The valence band is the highest range of electron energies in which electrons are usually found at 0 K temperatures. The conduction band on the other hand is the range of energy needed to free an electron from an atom and to turn it into a delocalized electron that can move freely in the atomic lattice. Electrons can move from the valence band to the conduction band with for example heat energy or energy acquired from a photon through excitation. The energy between these bands is called the band gap. The size of the band gap determines whether the material in question is a metal, a semiconductor or an insulator. This is illustrated in Figure 2.2. (Kumar & Chand 2012, Hoffmann 2008)

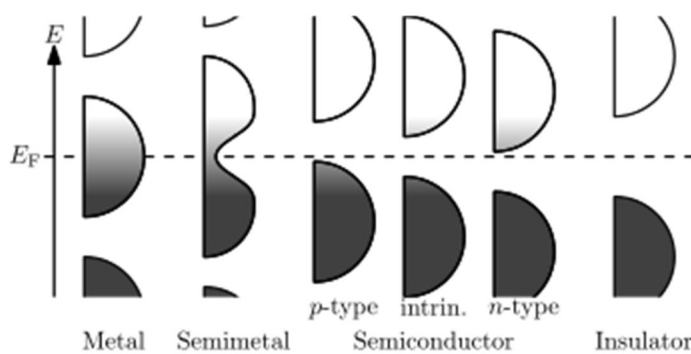


Figure 2.2. The characteristic difference in band gaps for various materials. (http://en.wikipedia.org/wiki/File:Band_filling_diagram.svg)

2.1.1 Different types of organic solar cells

There are many kinds of organic solar cells starting from the simplest single-layer cell to the very complicated tandem solar cells. Usually with complexity comes better performance. Still it is important to remember that organic solar cells do not (yet) compete with semiconductor cells in power conversion efficiency but in cost effectiveness. The more complex the cell architecture is the more difficult and therefore costly it will be to manufacture them. So in the end it probably won't be the most complex and effective solar cells that compete with inorganic solar cells, but some of the simpler and more cost-effective ones.

In single layer cells there is only a single light-absorbing layer between the two cathodes. The efficiency of these kinds of cells is much limited by the exciton diffusion length. Since the distance the exciton needs to travel to get to an interface where it could break into electrons and holes is the width of the entire cell, the cell film thickness remains very low, only around few hundred ångströms. So thin films are not thick enough to absorb much light and the cells are not very effective. (Kumar & Chand 2012)

Bilayer solar cells are one step more advanced. In them there are two layers of photoactive organic material, the acceptor and the donor. The two materials being separate allows for a much thicker film that can still transport electrons and holes and generate a potential. The distance excitons have to travel to the closest interface is now only half of the cells width. Regardless, the exciton diffusion length is a limiting factor in this architecture as well and film thickness still cannot reach optimum for absorption. Still efficiencies of up to 5.8 % have been achieved with these kinds of cells. (Kumar & Chand 2012)

Another step up the complexity ladder and we get the bulk hetero junction organic solar cell. The structure of a bulk hetero junction organic solar cell is presented in Figure 2.2. In this type of cell the acceptor and donor material are mixed together to form an active layer. This way the closest interface for the excitons to reach is very close and the exciton diffusion length is no longer a problem. This time the problem is the materials that can be used to form this kind of a structure. Not only do the materials need to be efficient light absorbers they also need to be able to be mixed and deposited together. The deposition conditions are very important as nanolevel configurations have a big effect on cell performance. Annealing after deposition can also affect the final cell tremendously. Finding new and better materials for these kinds of cells can still improve their performance from the 7.4 % achieved by 2012. (Kumar & Chand 2012)

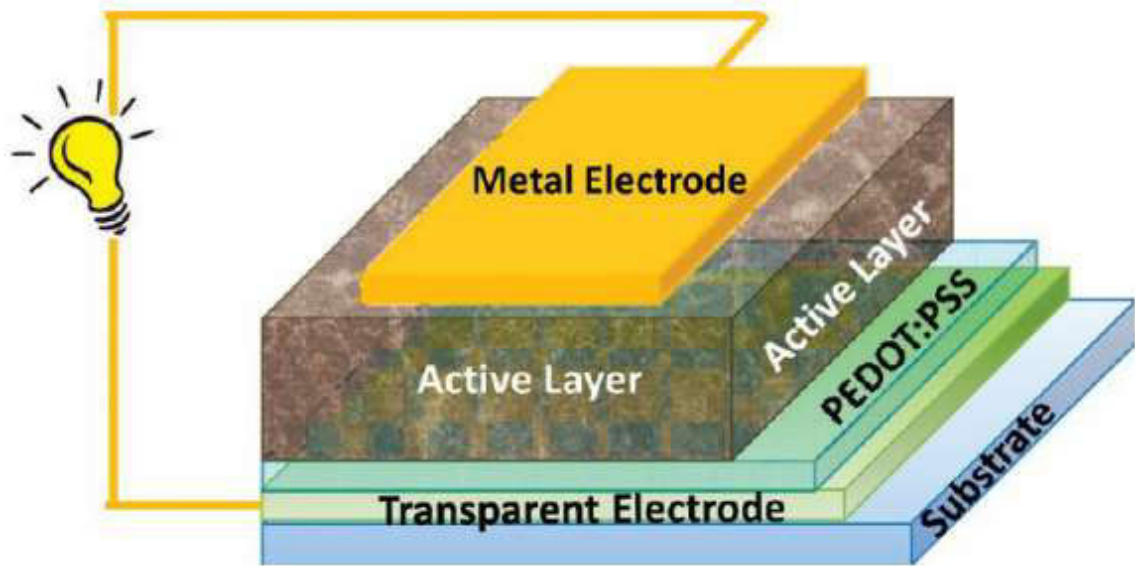


Figure 2.3. The structure of a bulk heterojunction organic solar cell. (Zhou et al. 2012)

Hybrid planar-mixed heterojunction cells are like the name indicates a hybrid between planar and bulk heterojunction solar cells. A similar layer as in bulk heterojunction solar cells is sandwiched between ETM and HTM layers as in bilayer solar cells. This accomplishes adequate cell thickness for absorption and efficient charge carrier transport. The cell can be quite thick as dissociation of the excitons takes place everywhere in the bulk hetero layer as well as at the surfaces of the ETL and the HTL. Exciton diffusion length is no longer an issue and the donor and acceptor materials are addressing charge carrier mobility, but still the diffusion lengths should be longer than individual film thicknesses. Cells of this type have not yet been perfected and even though the idea seems promising the best cells of this type reported by Kumar & Chand are not as efficient as the best bulk heterojunction cells.

In tandem solar cells two cells are combined to form a single cell. This is done because the band gap of a material is determined by the longest wavelength it absorbs and the longer the wavelength the lower the photon energy and therefore also the maximum V_{oc} and PCE achievable. On the other hand the wider the absorbance spectrum the more excitons are formed and the greater the current generated. The solar spectrum is divided into parts each part having a single absorbing material. The structure is so that the anode of the top cell should function as a cathode for the bottom cell. More than two cells can be combined, if suitable absorbing materials and anodes and cathodes are found. Proper combinations of different materials can achieve higher efficiencies than the respective cells would provide alone. Finding proper materials for this kind of cells is an issue though. It has been suggested that perovskite solar cells, the key interest of this work, could work well in tandem with silicon semiconductor solar cells. (Kumar & Chand 2012, Green et al. 2014)

Another type of organic solar cells is the p-i-n solar cells. In between p-doped and n-doped layers of inorganic semiconductors there is an intrinsic layer of an organic

photoactive material. The name comes from this configuration, p-doped, intrinsic, n-doped. These cells are not truly purely organic solar cells rather a hybrid. The n- and p-doped layers improve cell performance just like other layers utilised in many organic solar cells, but unlike them these layers are very efficient charge transporters. This type of a hybrid might very well be an important step in finding a cost-effective and easily manufactured way to produce energy for all. (Kumar & Chand 2012)

The cells studied in this work don't really fall into any of the above categories. The light absorbing materials in the finished cells are organo-metal halides. An organic ion forms the material together with a metal and three halides. More specifically the organic ion is methylammonium, the metal is lead and the halide is either iodine or chlorine. Along with this organic-inorganic light absorbing layer there is a scaffolding layer of mesoporous titanium dioxide, a blocking layer of TiO_2 , a layer of fluorine doped tin oxide (FTO) and a gold electrode. All of this is assembled on a glass substrate. In the same kind of cells as in this work, perovskite solar cells, various other materials are used as well. The organic part has been varied and bromide (Green et al. 2014) has also been used as the halide and some cells have been assembled onto bendable plastics such as polyethylene terephthalate (PET)/ITO. Despite the fact that these cells have seemingly very little organic material in them, they still function like organic solar cells and are relatively easy to manufacture and the absorbing material is cheap. Despite cheap absorbing materials the complete cells are still rather expensive because applying contacts to the cells and encapsulating them is expensive. The cells are really a type of organic-inorganic hybrid solar cells. Perovskites are not, at least not yet, the most effective types of cells, but their advancement has been the most rapid as shown in Figure 2.4. To date the best unconfirmed efficiency reported has been 20.1 % (Green et al. 2015) and the best independently confirmed PCE has been 17.9 % (Snaith 2013)

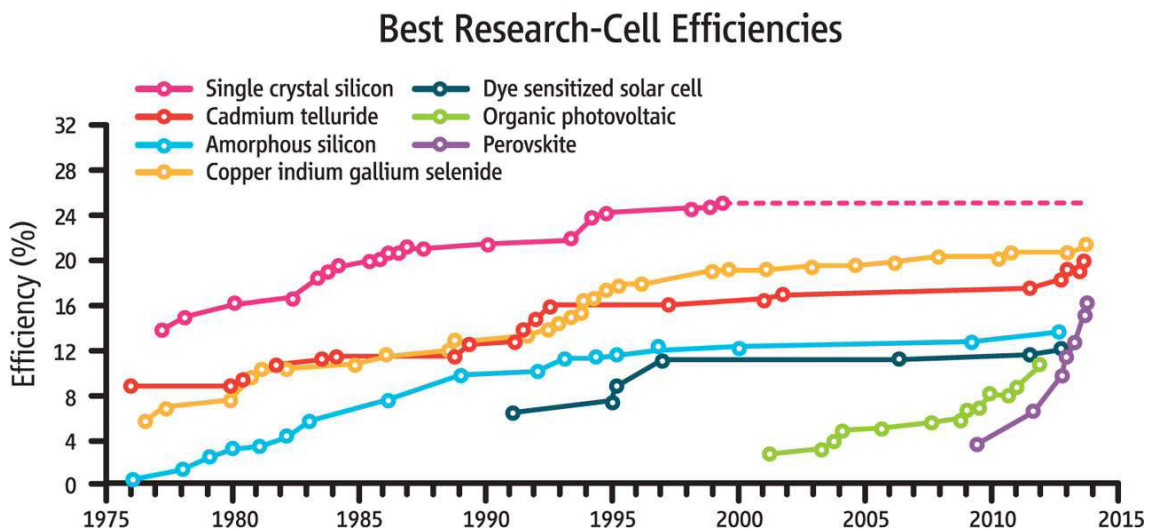


Figure 2.4. Comparison of reported highest efficiencies for various types of solar cells. (Service 2013)

2.1.2 Characterization of the cells

The efficiency of an organic solar cell means the ratio of electrons per unit time per unit area leaving the cell to incident photons per unit time per unit area. It can be measured by performing a so-called I-V measurement. In an I-V measurement a bias voltage is fed to the cell and current is measured as the bias voltage is being increased. The measurement curve tells directly the short-circuit current when the bias voltage is zero and the open-circuit voltage when the measured current is zero. The acquired short-circuit current is then divided by the electrode area, which is the actual active area of the solar cell. This is called the current density and the most commonly used unit for it is mA/cm². Also the maximum power point is easily obtained from such a curve it being the point where the absolute value of the product of current and energy is the highest. Figure 2.4 shows an example of an I-V curve and Figure 2.5 an example of a processed curve. The fill factor is easily calculated with the knowledge of P_{max} , I_{sc} and V_{oc} as it is simply $P_{max}/I_{sc}V_{oc}$. The power conversion efficiency of a cell can be determined by the formula:

$$\text{PCE}\% = \eta = \frac{I_{sc} \cdot V_{oc} \cdot \text{FF}}{P_{\text{light}}}$$

When determining the PCE the irradiance of the incident light is almost always set to be $100 \frac{\text{mW}}{\text{cm}^2}$, as this value corresponds well to the average power of sunlight on Earth at middle latitudes and the average conditions in which the cells will be used once perfected for commercial production and it is known as AM 1.5. AM stands for air mass and $\text{AM} = \frac{1}{\cos(\theta)}$, where θ is the angle of the Sun from its zenith. AM 1.5 is the standard according to which most solar cells are tested nowadays.

All measurement principles for photovoltaic solar devices used on the surface of Earth, including the AM 1.5G mentioned and used here, are defined in standard IEC 60904-3, Ed. 2, 2008. (Gueymard et al. 2002; Kumar & Chand 2012)

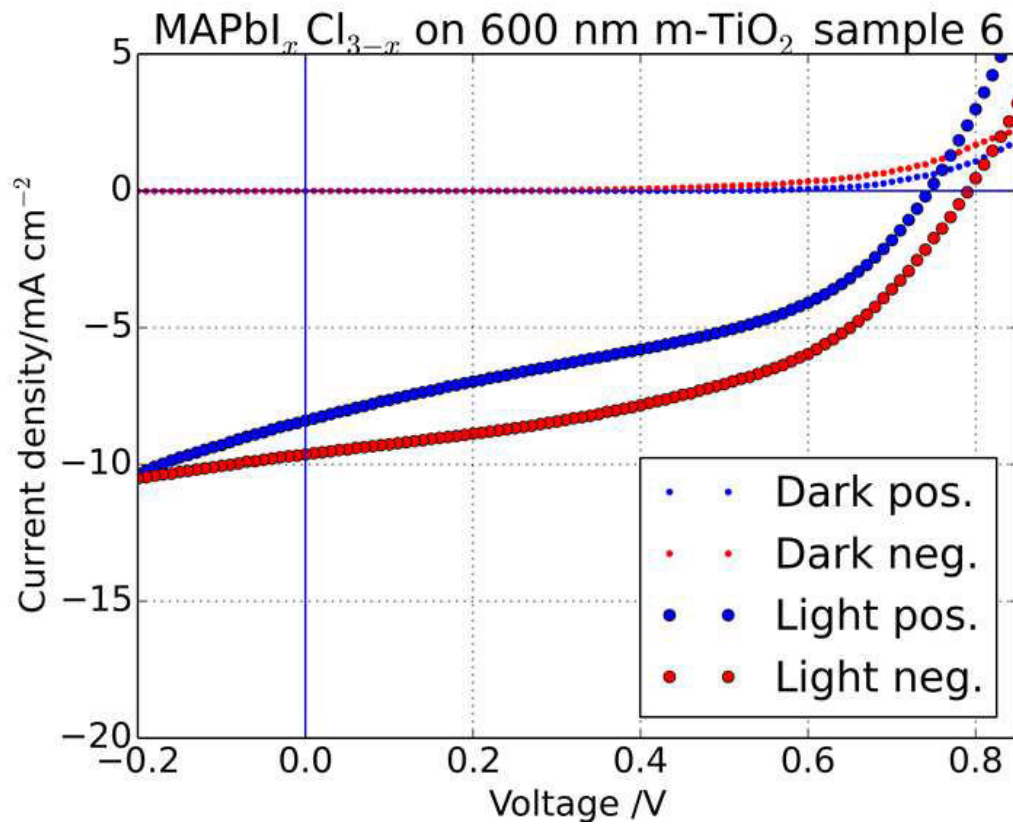


Figure 2.5. An example of an I-V curve taken of the last set of samples made for this work. The measurement was done once without illumination and once with illumination on both occasions the scan was performed in positive and negative scan directions to monitor possible hysteresis effect.

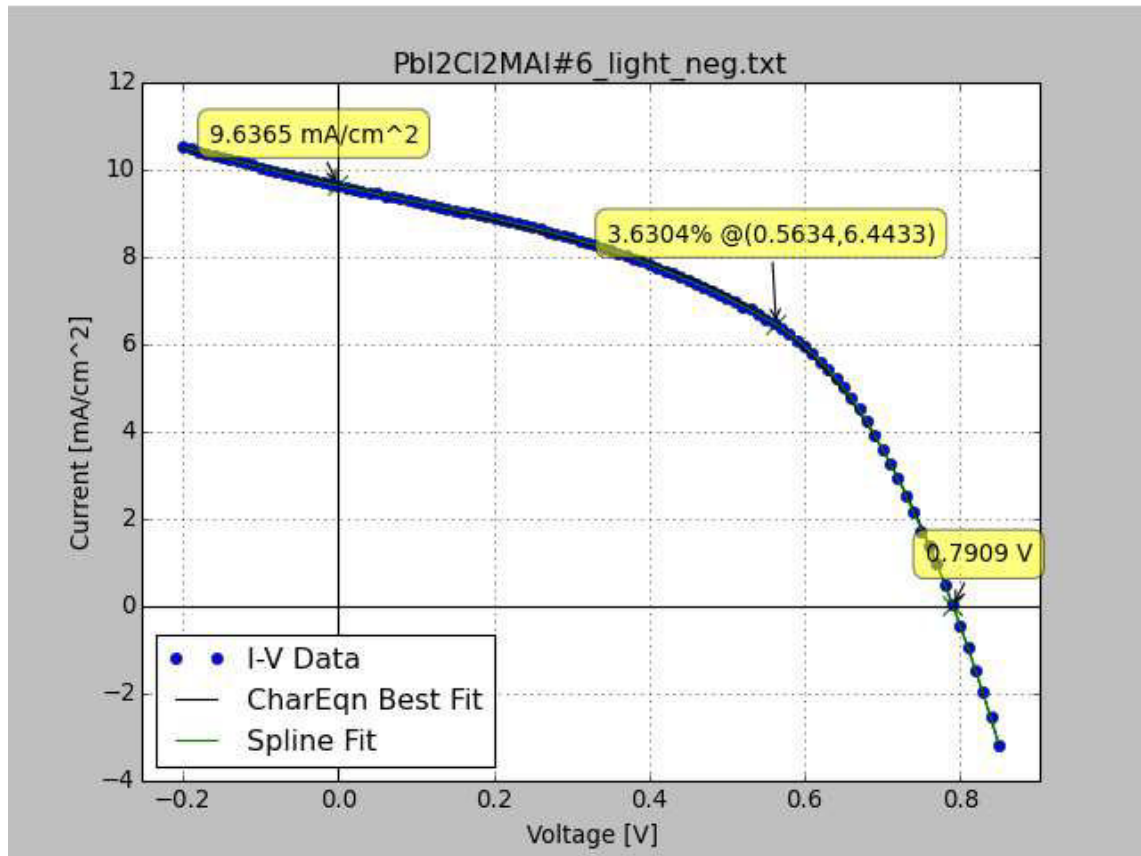


Figure 2.6. A processed I-V curve from the same data as in Figure 2.4, which shows P_{max} , V_{oc} , I_{sc} and PCE clearly. The current values have been multiplied by -1 to make for a clearer presentation.

Short-circuit (I_{sc}) current is the maximum current that a cell can produce. Open-circuit voltage (V_{oc}) is the maximum voltage that a cell can produce. Maximum power point (P_{max}) is the point on the I-V curve, where the absolute value of the product of current and voltage is the highest. Fill factor (FF) is the ratio of maximum power point to the theoretical maximum power of the cell, if open-circuit voltage and short-circuit current had their highest values in the same point. Power conversion efficiency (PCE) is the ratio of output energy to input energy. The characteristics listed above are the most important and most commonly reported characteristics, but there are other interesting ones that can be derived from the same I-V measurements. Spectral Response $S(\lambda)$ is the ratio of short-circuit current at a given wavelength to the photon flux at the same wavelength. External Quantum Efficiency (EQE) aka Incident Photon to electron Conversion Efficiency (IPCE) is given by the following equation

$$EQE = \frac{hc}{q} \frac{J_{sc}(\lambda)}{P(\lambda)\lambda^2}$$

Where h is Planck's constant, c is the speed of light, q is the elementary charge, λ is the wavelength and $P(\lambda)$ is the incident optical power at a given wavelength. Internal Quantum Efficiency (IQE) can be calculated from this by taking loss factors into account. Shunt Resistance is a desired characteristic of a solar cell. If shunt resistance is

small then fill factor is likely to be bad as well. When shunt resistance is small a significant part of the charge carriers finds a shorter shunt pathway thus avoiding the actual cell and reducing the cell's efficiency. A poor shunt resistance is most often due to manufacture defects rather than poor cell design. (Kumar & Chand 2012)

2.2 History of perovskite

Perovskite is a name for the mineral calcium titanate (CaTiO_3), but it also lends its name for a large variety of crystals with the same crystal structure as calcium titanate. The mineral was first discovered in 1839 by a German geologist in the Ural Mountains in Russia and named after a Russian geologist Lev Perovski. Perovskites consist of two different anionic ions and three cationic ions of the same kind. One of the positive ions has a charge of 2+ and the other a charge of 1+, while the negative ion type has a charge of 1-. This transfers to the general formula of MAX_3 . This formula is of course only the simplest form and perovskite structures form with more complicated formulas as well, for example $\text{YBa}_2\text{Cu}_3\text{O}_{7-x}$, which is a high temperature superconductor. Even though their structure appears simple enough, various perovskites exhibit a plethora of different attributes. Mostly they show these qualities only under special circumstances, if for example the perovskite has undergone some kind of structural distortion. Since their discovery and the characterization of their crystal structure they have been widely studied and their tunable attributes have been implemented on many fields of science. (Lotsch 2014)

Perovskites were first used in photovoltaics by Miyasaka et al. in 2009. They made photocells with a liquid phase electrolyte based on mesoporous TiO_2 photoanodes sensitized with $\text{CH}_3\text{NH}_3\text{PbX}_3$ ($\text{X}=\text{I}, \text{Br}$). They achieved an average PCE of 3.8%, which in comparison with other fields at the time was not very impressive, and the cells had very poor stability, but with a very V_{oc} of almost 1V they sparked the interest of the scientific community. Three years later in 2012 Kanatzidis et al. created a dye sensitized solar cell with CsSnI_3 as a p-type semiconductor. This all inorganic all solid-state cell achieved a PCE of about 10% and managed to spark new interest in its field. (Lotsch 2014; Green et al. 2014)

2.3 Preparation methods of perovskite solar cells

In this chapter some of the most common ways to fabricate perovskite solar cells are described. All the methods use similar materials and result in comparable cells and cell performance. The ones in this work were mostly made via the two-step deposition method aside from a batch that was done by the single-step preparation method. These methods have also been combined and it is hard to align some work to only one of these categories. Some of the preparation methods are illustrated in Figure 2.8. The methods are then discussed in more detail in the following paragraphs.

Perovskite solar cells are usually assembled on glass substrates coated with for example FTO or ITO. On top of the doped tin oxide there is usually a layer of compact

TiO₂ and on top of that a mesoporous layer of the same. Then within and on top of the mesoporous layer there is the photoactive layer of perovskite. On top of the perovskite there usually is a layer of hole conducting material such as Spiro-OMeTAD and then finally a gold electrode. The structure of a typical perovskite cell is depicted in Figure 2.7.

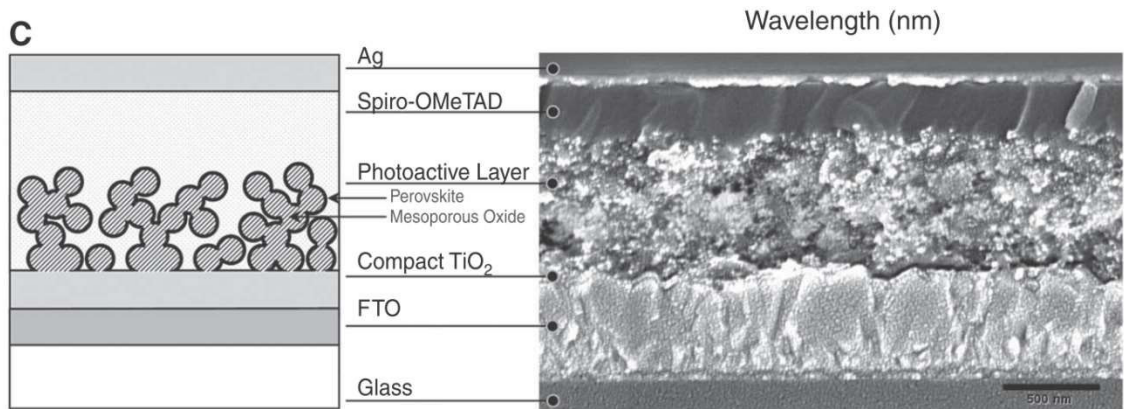


Figure 2.7. The structure (left) and SEM-image (right) of a typical perovskite solar cell. (Lee et al. 2012)

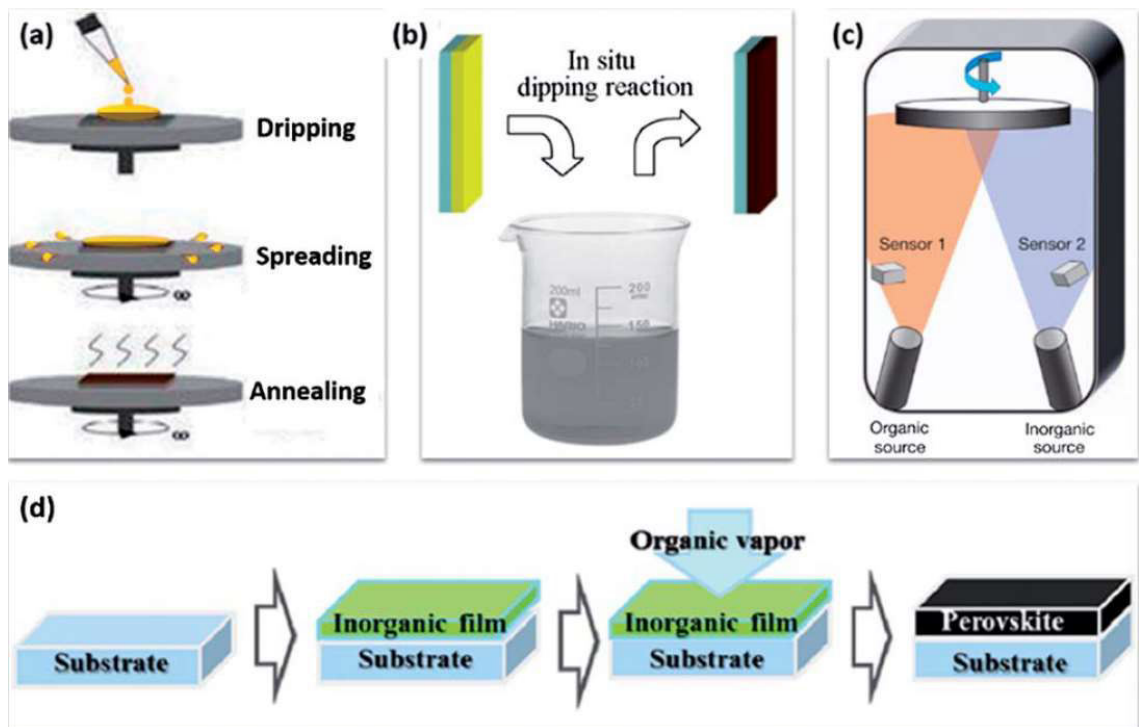


Figure 2.8. Four of the most common preparation methods; a) one-step precursor deposition; b) sequential deposition method; c) dual-source vapour deposition; d) Vapour assisted solution process. (Gao et al. 2014)

2.3.1 One-step precursor deposition

In the one-step precursor deposition method all the precursors of the perovskite are dissolved in a common solvent in the same solution. This is the most widely used method to prepare perovskites due to it being also the simplest. Solvents used include DMF and γ -butyrolactone. A sufficiently high amount of perovskite precursors like PbI_2 and MAI is dissolved in the solvent and then this solution is spin cast onto a suitable substrate. The mass-% of the solution should be around 40% otherwise the perovskite film formed will be inconsistent. After the deposition the substrate is annealed to finalize the perovskite formation process. Then on top of the perovskite an optional hole conducting layer is deposited. The process might include other nonessential phases and components as well. A top all the layers in between an electrode is deposited usually via thermal deposition. The electrodes are often of gold or silver. This method was used in making seven of the 39 solar cells made during this work. (Gao et al. 2014)

2.3.2 Sequential deposition method

In the sequential deposition method first the lead halide or a mixture of lead halides is dissolved in a solvent like DMF or γ -butyrolactone. This solution should again be strong enough to ensure good coverage of the substrate in the following spin coating phase. After the substrates have been spin coated they are annealed to evaporate all residual solvent. A solution with the other precursor of the desired perovskite is made into a solvent that does not dissolve perovskite or the other precursor. The substrates are then after annealing dipped in this solution to allow the perovskite formation to take place. Normally no annealing is required to finish the perovskite formation as the process is almost instantaneous. After the desired dipping time has passed, the slides are removed and annealed again to remove any residual solvent. Once the solvent has evaporated additional layers may be added to the cell and once again the final part is the metal electrode. This method gives better control over the perovskite morphology than the one-step precursor deposition method and film morphology is one of the key factors in perovskite cell performance. (Burschka et al. 2013)

2.3.3 Dual-source vapour deposition

As the name indicates in this method the perovskite precursors are vaporised and the substrate is placed so that the both vapours meet it and form a highly uniform film on it. Once the film is formed additional may be applied just as with the other methods. This method is not as low cost as the other two described so far, but the uniformity of the films produced might just make up for it. The uniformity of the film makes for increased cell efficiency. (Liu et al. 2013)

2.3.4 Vapour assisted solution process

This method is actually a combination of the sequential deposition method and the dual-source vapour deposition. The lead halide is spin coated on the substrate just like in SDM and then the methylammonium iodide or other similar molecule is vaporised on it to form the perovskite. In the case described more closely the lead halide was PbI_2 and the substrate was FTO with a compact layer of TiO_2 . On top of this MAI was vaporised at 150°C in a N_2 -atmosphere for two hours. The films formed had reportedly full coverage and similar grain structure. Both of these things are considered beneficial for cell performance. (Gao et al. 2014)

2.4 Perovskite properties

Perovskites have a lot of interesting properties and they have been used in various fields of science for many things. The perovskites used in photovoltaics are semiconductors, but other materials with the same kind of crystal structure also labelled as perovskites have uses as insulators, conductors and even superconductors. In this work the focus is on photovoltaic exploits of perovskites, so they are ones to be delved into in more detail. These perovskites exhibit large absorption coefficients in the visible region as seen in Figure 2.9. A large absorption coefficient is vital for photoactive materials in solar cells. (Service 2014)

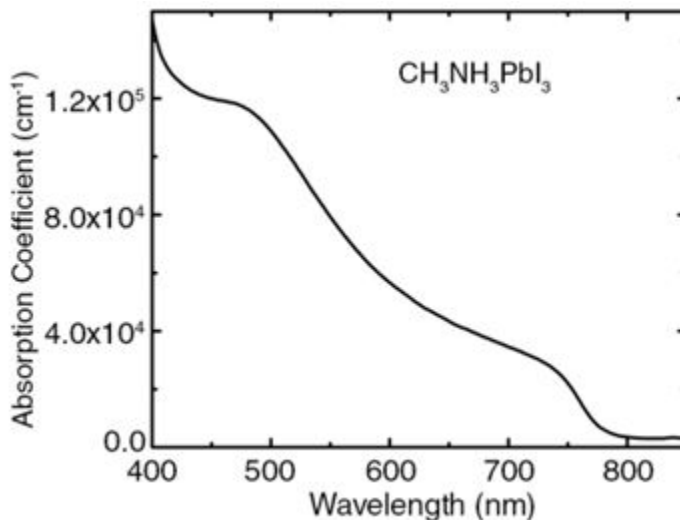


Figure 2.9. Absorption coefficients of methylammonium lead iodide perovskite as a function of wavelength. (Xing et al. 2013)

2.4.1 Crystal structure

Figure 2.10 shows the cubic crystal structure of perovskites. Perovskites exhibit other crystal structures as well the orthorhombic in temperatures below -112°C and the tetragonal in temperatures between -112°C and 56°C . The tetragonal structure is along

with the cubic for photovoltaic the most important as these fall into the temperatures where solar cells would be used. The tetragonal perovskite crystal structure is shown in Figure 2.11. (Juarez-Perez et al. 2014)

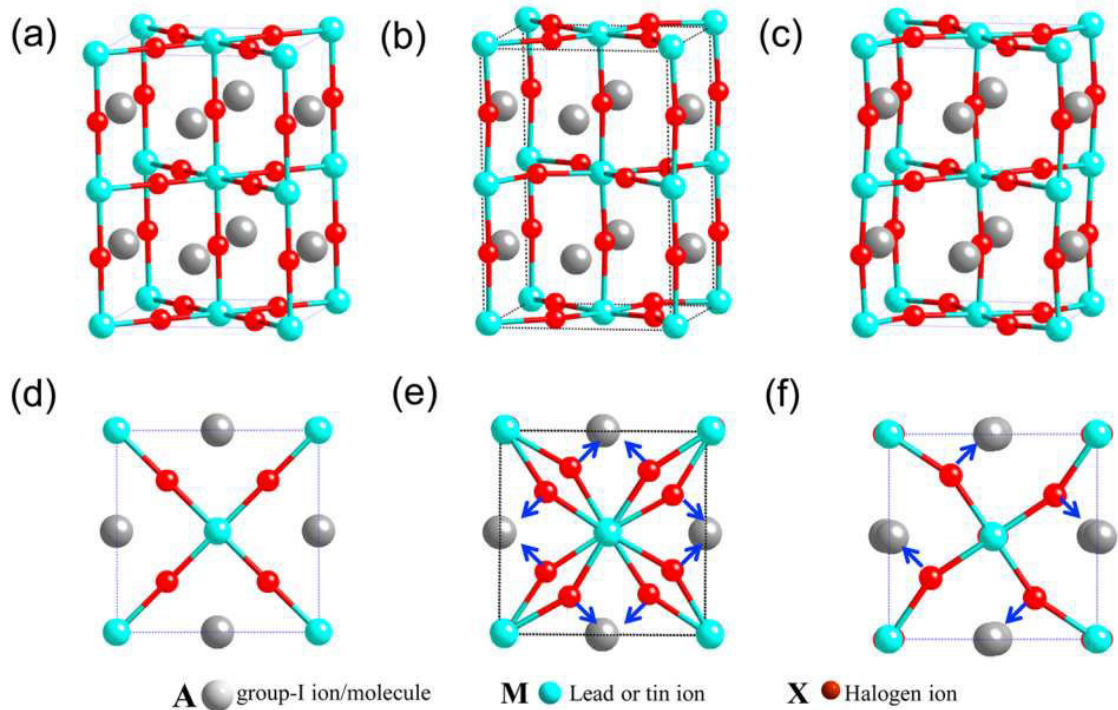


Figure 2.10. The crystal structure of a) α - b) β - and c) γ -perovskite d)-f) are the same types as viewed from the top. (Yin et al. 2014)

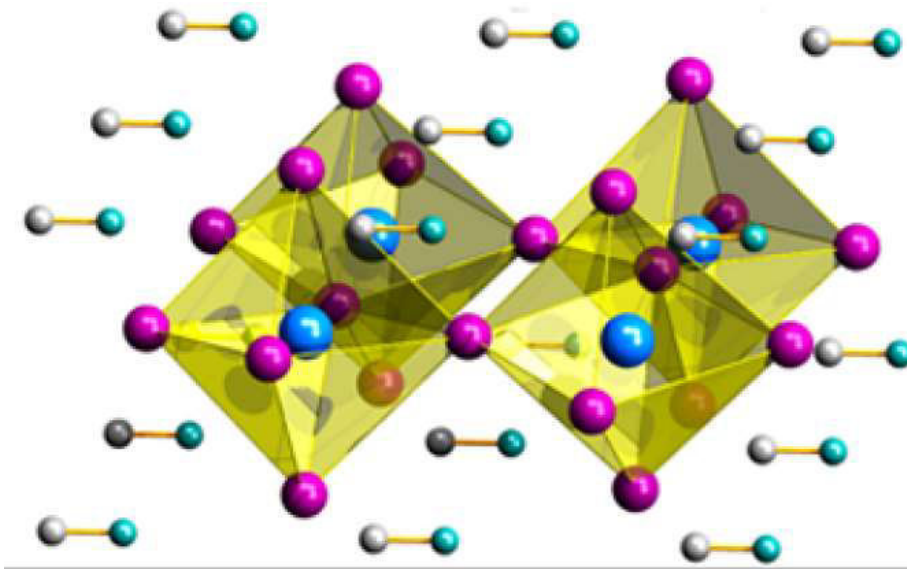


Figure 2.11. Tetragonal perovskite structure, the blue sphere is the B cation (Pb^{2+}), the crimson spheres represent the X anion, and white and cyan spheres represent C and N atoms from MA. (Juarez-Perez et al. 2014)

2.4.2 Energy level

Methylammonium lead bromide perovskite has its valence band at 5.38 eV and its conduction band at 3.36 eV below vacuum level. $\text{CH}_3\text{NH}_3\text{PbI}_3$ has its valence and conduction bands at 5.44 eV and 4.0 eV respectively. In comparison the conduction band level of titanium dioxide is 4.0 eV. The band levels of other materials can be seen in Figure 2.12. (Kojima et al. 2009)

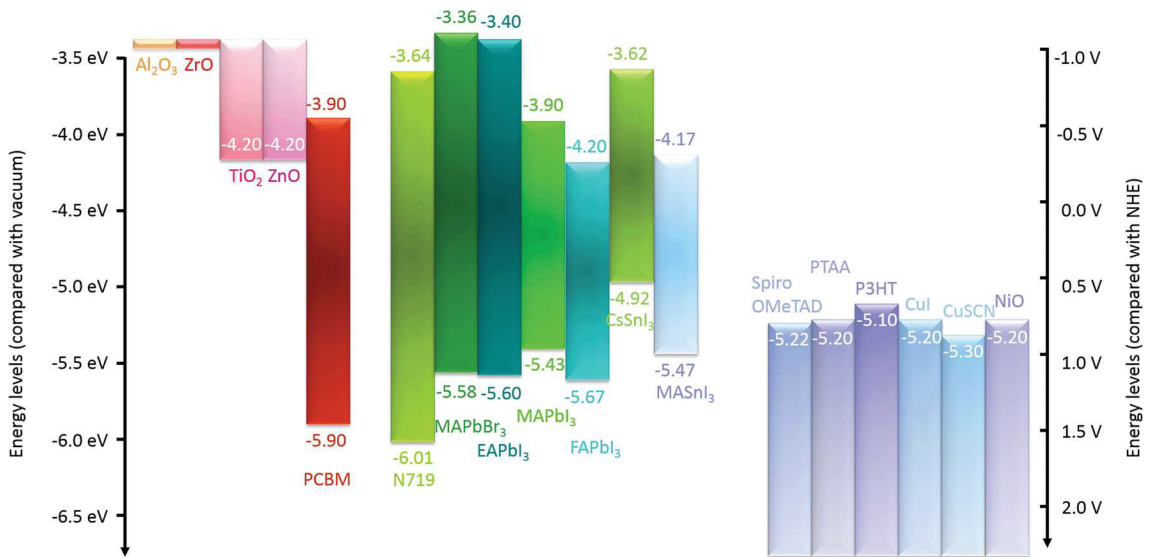


Figure 2.12. Band levels of various materials relevant to perovskite solar cells. (Gao et al. 2014)

2.4.3 Charge carrier properties

In methylammonium lead iodide perovskite, electron-hole pairs are generated almost instantaneously and they dissociate forming highly mobile charge carriers. The electron and hole mobilities are almost balanced and remain very high up to the microsecond time scale. The maximum mobility value achieved for $\text{CH}_3\text{NH}_3\text{PbI}_3$ by Ponseca et al. (2014) was $25 \text{ cm}^2\text{V}^{-1}\text{s}^{-1}$. In comparison for charge carrier mobilities for Si are in the range of $450 \text{ cm}^2\text{V}^{-1}\text{s}^{-1}$ for holes and $1400 \text{ cm}^2\text{V}^{-1}\text{s}^{-1}$ for undoped silicon with the mobilities decreasing with increasing levels of doping density. (Van Zeghbroeck 2011) Perovskite falls short of this, but when compared with organic semiconductors the values are decent. According to Coropceanu et al. (2007) crystalline organic semiconductors reach charge carrier mobilities in the range of $0.1\text{-}20 \text{ cm}^2\text{V}^{-1}\text{s}^{-1}$ and in amorphous materials the mobilities remain below $0.1 \text{ cm}^2\text{V}^{-1}\text{s}^{-1}$. If the perovskite is in a TiO_2 mesoporous structure, electron injection from the perovskite is effective in less than a picosecond. However titanium dioxide has intrinsically lower electron mobility and this

leads to an unbalanced charge transport. The decay of mobile charges in $\text{CH}_3\text{NH}_3\text{PbI}_3$ is very slow and lasts up to tens of microseconds. These properties make $\text{CH}_3\text{NH}_3\text{PbI}_3$ a remarkable material for photovoltaics. If a metal oxide with higher electron mobility can be found, the potential performance of perovskite solar could rise even higher. (Ponseca et al. 2014)

3 EXPERIMENTAL

The time window for this work was relatively short. Therefore one of the simplest types of perovskite cells was chosen to be the focus of the work. Four sets of cells with more or less the same approach were made. After each set, some parameters were altered according to observations made and ones found in the literature. The first set of cells gave a poor result and most of the cells did not work at all, but in the 4th set the best results were already comparable to others in the literature. The 4th set still had a lot of variance in the cell properties. Between the 16 cells in the set the efficiencies varied from 1.5% to 7.9%. Various other experiments were tried as well along with the solar cell sets.

3.1 Cutting glass

All the glass slides used in these experiments were cut by drawing a straight line on the desired cutting area with a diamond pen and then bending with gloved hands. Most of the slides broke in the desired point, but some variation occurred and all of the edges were not straight.

3.2 Lead Iodide films on glass substrates

The first experiments were done on glass slides to get more familiarity with the methods to be used in making the actual solar cells while not wasting solar cell substrates that needed to be ordered from Solaronix SA, Switzerland. Four glass slides with dimensions of approximately 26mm*26mm were cut from larger glass slides (76mm*26mm). The slides were numbered with a diamond pen. These slides were then thoroughly cleaned. First the slides were bathed and sonicated in chloroform for 20 minutes at maximum power. After chloroform they were bathed and sonicated in Helmanex III 2% solution, Sodium Dodecyl Sulphate 1M and MilliQ water, 20 minutes in each. Between each step the slides were rinsed with MilliQ water. After the last sonication the slides were set in an oven to dry at 150 °C for 60 minutes. After this the slides were stored in a Gram stainer overnight. A Gram stainer at a later stage of the work is depicted in Figure 3.1. The next morning the slides were further cleaned with a Harrick Plasma PDC-002 plasma cleaner for ten minutes at high plasma level.

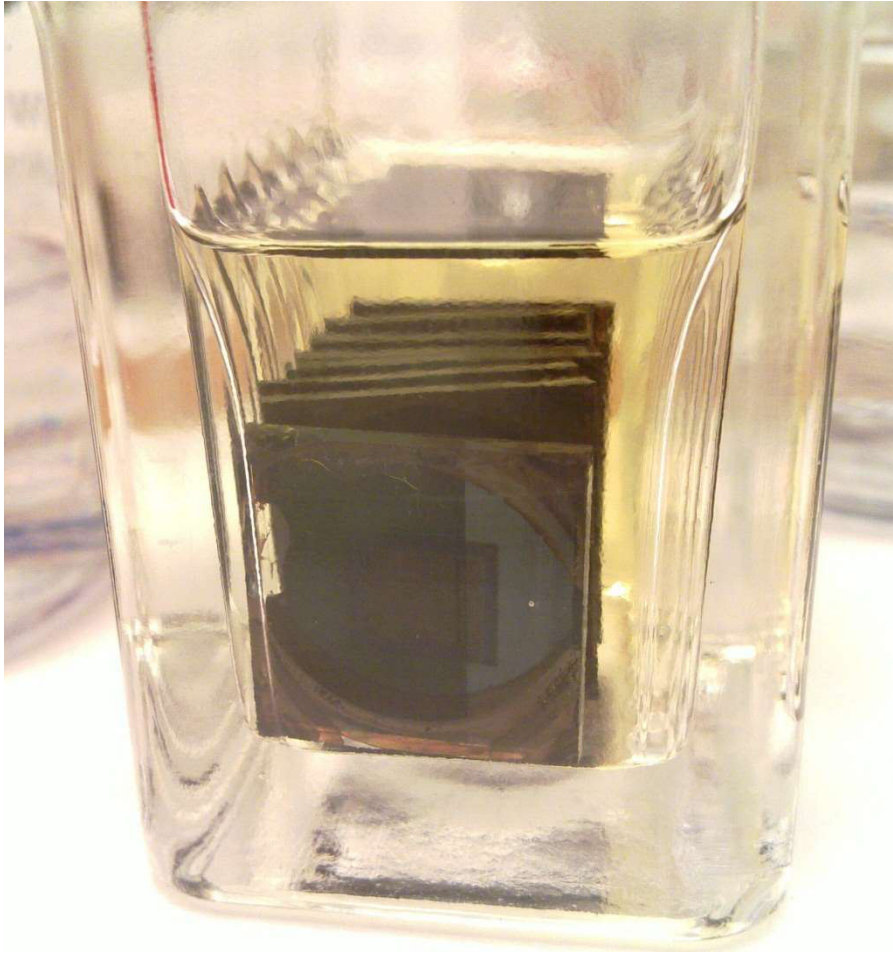


Figure 3.1. *A Gram stainer with methylammonium lead iodide perovskite solar cells in the making.*

A solution of PbI_2 was prepared. The desired concentration was the same as used by Shi et al. (2014a), 1.2M. 2.75g of PbI_2 was weighed using an analytical scale. The PbI_2 used was 99,999% pure from Sigma Aldrich. The substance was grainy. 5 ml of N,N-dimethylformamide was added to the substance and it was set on a heater plate with a magnetic stirrer. The temperature was set at 75 °C. The PbI_2 did not dissolve readily and therefore it was left on the stirrer without heating overnight. In the morning the PbI_2 was an almost solid block. The PbI_2 was sonicated for 7 minutes and ended up looking like powder. 2 ml of DMF was added to get the PbI_2 to dissolve. When the solution with added volume was set on a heater plate with a magnetic stirrer, the PbI_2 dissolved nicely. The resulting solution had at least a 0.857 mol/l concentration. The concentration might be higher as part of the solvent might have evaporated during heating and stirring.

The thoroughly cleaned slides were spin coated with the PbI_2 solution. A Laurell technologies corporation model WS-4003-6NPP/lite spin coater was used. 200 μl of PbI_2 solution was administered in the centre of the slide and the slide was spun for 60 seconds at 2000 rpm with an acceleration of 1:00. After spinning, the slides were col-

lected on a sheet of aluminium foil and once all the slides had a coating they were set on a heater plate at 90 °C for three minutes. Then the absorption spectra of the slides were measured using a Shimadzu UV-3600 UV-VIS-NIR spectrometer. After measuring the absorption spectra, another coating of PbI_2 was added and the spectra were measured again. According to two different papers from Shi et al. (2014a and 2014b) a single layer of lead iodide is not enough to get a good film coverage. After measuring the absorption also emission was measured. The emission spectra were acquired with an Instruments S.A. Fluorolog.

Two of the slides were protected with smaller glass slides cut from microscope glass. The protective slides were adhered with 100 μm thick thermoplastic Meltonix-polymer from Solaronix. A piece of the same size as the protective slide was cut from the larger Meltonix foil and a small window, the size of the active area in the solar cells, was cut. The area around the active area was cleaned with a cotton stick dipped in ethanol so that the Meltonix would stick better. First the Meltonix was melted on the protective slide on a hot plate at 105 °C in air. Once the slides had cooled down the protective polymer was removed from the Meltonix windows and the glass slides were deposited on the samples so that the Meltonix touched only areas cleaned with the cotton stick. The samples were then moved with two steel nuts as weights on top into an exicator with a hot plate. A vacuum was pumped and the chamber was flushed once with nitrogen so that most if not all of the oxygen and water in air exited the chamber. Then the hot plate was turned on and set to warm to 105 degrees. The samples were left in the exicator for 45 minutes after which the heat was turned off and the samples were left to cool down in vacuum. The Meltonix melted and affixed firmly on both the sample slide and the protective slide. A set of solar cells being sealed can be seen in Figure 3.2.



Figure 3.2. Solar cells being sealed.

The two slides, which were not covered with the protective glass, were dipped in a methylammonium iodide solution with 2-propanol as solvent and a concentration of 10 mg/ml. The methylammonium solution appeared initially colourless, but after a few hours the colour started changing towards yellow and after a sufficient amount of time even a rather intense yellow. The slides were kept in the solution for one minute. In this time a methylammonium lead iodide perovskite was formed on the slide. The slide visibly changed colour from greenish-yellow to greyish-black in the first few seconds. The slides were photographed with a microscope. The slides were set in an exicator to dry for 60 minutes at 90 °C. After the drying the slides were photographed again, but no notable change was observed. Of these newly formed perovskites absorption, transmittance, reflectance and emission spectra were measured. The spectra will be discussed in greater detail in the results section (section 4) of this document.

3.3 First set of solar cells

The substrates for the first solar cells were ordered from Solaronix SA, Switzerland. There were two kinds of substrates, 4 of each. Both were of glass and had an etched FTO-coating and a dense blocking layer of TiO_2 about 50 nm thick. On top of this one kind had a 300 nm thick mesoporous layer of TiO_2 and the other had a 600 nm layer of

mesoporous TiO₂. A schematic picture of the substrates from Solaronix can be seen in Figure 3.3.

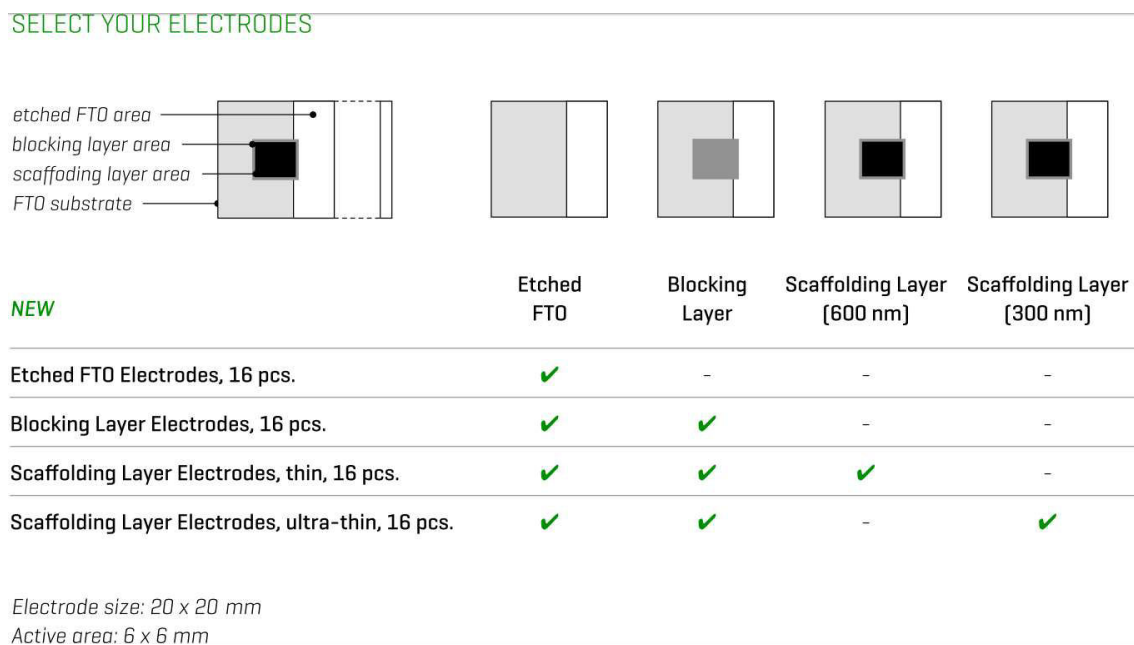


Figure 3.3. A schematic picture of the substrates from Solaronix. (http://www.solaronix.com/documents/solaronix_materials.pdf)

Lead iodide was spin coated on the slides in two layers the same way as was done with the slides of microscope glass previously, except that these slides were not cleaned to prevent possible damage to the delicate structures of the substrates. Absorption spectra were measured after each step of preparation.

After spin coating the slides were dipped in a 10 mg/ml methylammonium iodide solution. The solvent of the solution was isopropanol. Just like with the glass slides also these substrates underwent a rapid and visible change. The colour of the film changed from greenish-yellow to greyish-black. The visible part of the reaction was over in seconds and no change could be observed during the rest of the minute that the slides were kept in the solution. The slides were photographed with a microscope and then put in an exicator for 60 minutes at 90 °C and then photographed. Like with the glass slides the substrates didn't look any different after the baking. The absorption, transmittance, reflectance and emission spectra of the slides were measured. Two cells of each kind were covered with a protective glass slide affixed with Meltonix. The procedure of covering the slides was identical to the one described in chapter 3.1 used for glass slides. The I-V-curves of all the cells were measured.

3.4 Measuring I-V curves

All of the I-V measurements for this work were carried out with a setup that had a model 66921 Xenon-lamp from Newport and measurement units E5272A and E5281A from

Agilent Technologies. The light from the lamp was filtered with a 315-710 nm band pass filter (FGS900S, Thorlabs). The irradiance was measured with a reference cell from Oriel instruments. The model was 91150V. The samples were set in the same position, where the reference cell showed the power of one sun to match the AM1.5G standard, which was discussed earlier, as closely as possible. In reality the measurements are not entirely up to the standard, but close enough to make further research feasible. The curves themselves will be discussed in greater detail in the results section.

The electrode areas were measured to calculate the current densities needed to acquire the actual I-V curves. Each cell was pictured with a Dino-Lite AM4113ZTL microscope. With careful calibration of the microscope and a picture handling program called Fiji ImageJ (Schindelin et al. 2012) the area visibly covered by the electrode was encircled and the program calculated the area. The current values given by the I-V measurement were then divided by this area to get the current density.

3.5 Refining the process of making a uniform layer of perovskite

Slides of microscope glass were cut to squares with dimensions of approximately 26 mm*26 mm. Altogether 16 slides were cut. These slides were placed in two Gram stainers and underwent the same cleaning procedure as the first 4 slides. In addition to this cleaning, the slides were soaked in acetone under a fume hood for five days before drying and plasma cleaning.

New lead iodide was ordered from Sigma Aldrich. This time the purity was only 99 % instead of 99.999 %. The only reason, the extremely pure lead iodide was used in the first place, was a shorter delivery time. The 99 % pure lead iodide is pure enough for all purposes. Out of this lead iodide two solutions were prepared, one with a 0.6 mol/l concentration and another with 1.2 mol/l concentration. 1.39 g of lead iodide was weighed for the more dilute one and 2.76 g for the other one. Five millilitres of DMF was added to each and the vials were shaken and stirred. The lead iodide in the 0.6 M solution dissolved readily in room temperature, but the lead iodide in the other solution refused to dissolve even after more than 24 hours of magnetic stirring and heating to 75 °C. In the end 1 ml of DMF was added and the lead iodide dissolved rather readily. The resulting concentration was of course lower and taking in to account the DMF that had evaporated during the dissolving process, it was 0.999 mol/l.

With the newly prepared solutions of PbI_2 in DMF three experiments were carried out, one with the more dilute solution to see whether three coats with a more dilute solution would yield better results, and two with the stronger solution. Out of the two experiments with the stronger solution the first one was to determine whether scratching the microscope slide surface with sand paper would result in better aligned crystals and a higher overall coverage and the other to determine, if heating the slides, on which the solution was spin coated, just before spin coating would improve layer uniformity. In addition to the before mentioned changes also the amount of lead iodide solution deposited on the slide during spin coating was increased to 100 μl . The three experiments

were otherwise performed in the same manner as the ones before them, with the same settings of the spin coater and the spectrophotometer and the same devices.

3.6 Second set of solar cells

Another set of eight solar cells was made. According to the results from the previous experiment a stronger lead iodide solution was used and the substrates were heated on a hot plate prior to spin coating. The samples were numbered 9-16 to continue the series of solar cells with basically the same recipe. Samples 9-12 had a mesoporous titanium dioxide layer of 300 nm and samples 13-16 a layer of 600 nm. Of each group two samples had a dipping time of 60 minutes and the other had a dipping time of 120 minutes. The dipping was performed in room temperature in a Gram stainer as with the first solar cells.

The same lead iodide solution was used as for the lead iodide on heated glass slides. This solution was 0.001 M stronger than the 0.999 M used for the first set of cells, but still significantly lower than the 1.2 M reported by Shi et al. (2014). A 30 ml solution of methylammonium iodide was prepared for the dipping phase. 300.3 mg of MAI was weighed and mixed with 30 ml of 2-propanol.

All slides were spin coated twice with the strong lead iodide solution and after the second coating their absorbance spectra were measured. The spectra were measured again after being annealed at 90°C after dipping. Then the samples were stored in an exicator overnight and the next day gold electrodes were thermally evaporated using the same procedures as with samples 1-8. Dots of silver paint were again applied as well as the protective glass slide. The I-V curves of the samples were measured after the application of the protective slides.

3.7 Monitoring the decay of the solar cells and further experiments with the solar simulator

The IV-curves of the solar cells were measured several times and at least once a week. The effect of longer measurements under illumination on solar cell performance was measured using a single cell and various constant voltages for various amounts of time. To test this sample 10 was put to the test. The shortest measurements were 10 minutes while the longest was 100 minutes. After the first constant voltage measurements the cell degraded notably and the maximum power point voltage changed so the set bias voltage for the measurement was changed too. More analysis can be found in the results and discussion section.

3.8 Durability test

The durability of the cells and the effectiveness of the protective glass were put to the test. The idea for this test came from Habisreutinger et al. (2014). The protective glass was removed from sample 14 for SEM-imaging and this sample and sample 15 were put on a hot plate in 80 °C under a fume hood for an extended time. After 24 hours they

were pictured and the cover from sample 15 was removed. The cover from sample 13 was also removed and it was placed on the hot plate. Sample 16 was also put on the hot plate to still have a reference for protected samples. The three unprotected samples and the one protected one were left on the hot plate over the weekend. On Monday morning they were imaged once again. Also the absorption spectra and IV-curves of the cells were measured.

3.9 Perovskite tablets by pressing from powder

A perovskite powder was formed with basically the same method as with the solar cells and glass slides. One gram of lead iodide was ground with a mortar and a pestle and a rotating mill. The resulting very fine powder was then sprinkled in 50 ml of 2-propanol, which had 1,032 grams of methylammonium iodide in it. The molar ratio of lead iodide to methylammonium iodide was 1:3. The reaction is equimolar, but supposedly a surplus of methylammonium iodide facilitates the reaction. The powder turned instantly black and sunk slowly to the bottom of the flask. The absorption spectra of the methylammonium iodide solution were measured both before and after the immersion of lead iodide. The solution was diluted 1:3 to achieve an absorbance that was better in the range of the measurement device. No decrease in the peaks was observed. Therefore we concluded that most of the methylammonium had not reacted and the perovskite seen on the bottom of the flask was in fact lead iodide with a thin covering of perovskite. To allow more perovskite to form we attempted stirring with a magnetic stirrer and sonication. This improved the results somewhat, but still a lot remained unreacted.

The acquired perovskite powder was extracted from the solution via centrifuging. After centrifuging the 2-propanol in the tube was removed with a Pasteur pipette. More 2-propanol was added and the tube was shaken and the process was repeated, so that the methylammonium still in the solution and in between perovskite particles was washed away. The perovskite accumulated in the bottom of the centrifuge tubes easily enough, but probably due to small particle size it formed a black sludge, which was almost impossible to remove from the tubes. Approximately 400 mg of the perovskite was successfully extracted from the tube onto a Petri dish with a tiny metal spoon.

The acquired perovskite was set in an exicator to dry overnight. The next day the perovskite was scraped off the Petri dish and weighed on a plastic weighing boat. Then the perovskite was ground with a rotating mill and pressed into a tablet with a press normally used to make KBr-tablets for IR-spectroscopy. The pressure applied was approximately 9 tonnes so about 665 MPa. The perovskite pressed into a shiny and fragile tablet. The conductivity of the tablet was measured and it seems to be a semi-conductor. By attaching the tablet onto a glass slide with two-sided adhesive tape fluorescence measurements were made possible.

The rest of the perovskite that was left in the centrifuge tubes was left to sit in 2-propanol. On top of the perovskite in all the tubes a layer of lead iodide formed. The absorption spectrum of the 2-propanol was measured and it gave similar peaks as the ones measured from the methylammonium iodide solution. It would seem so that the

perovskite decomposes in 2-propanol and the methylammonium iodide dissolves in the liquid. Meanwhile the perovskite stuck in the walls of the tubes and exposed to air remained visibly the same. This would indicate that air is a more hospitable environment to perovskite than 2-propanol. The remaining perovskite was suction filtered using a blauband filter paper meant for slow filtering. A lot of the perovskite particles went through the pores of the filter paper, so the same liquid was filtered several times using the same filter paper. The filter paper was then set in an exicator to dry overnight.

174.5 mg of perovskite was harvested from the filter paper onto a Petri dish. Another attempt at pressing a tablet from perovskite was made. There being a lot less perovskite than on the previous attempt an all-too brittle tablet was formed and even after several attempts it proved impossible to retrieve it intact from the tablet press. An attempt at attaching a piece of silver foil to act as an electrode and a support for the tablet failed as well. The silver was cleaned in an ammonia solution and rinsed with MilliQ water before pressing. The silver foil did not become attached and the tablet was brittle and broke just like before.

Another attempt at the perovskite powder was made via a solid state reaction. 207.6 mg of PbI_2 was weighed directly onto a mortar followed by 113.1 mg of MAI. The two powders were ground together with the pestle. The perovskite formation reaction did apparently take place as the yellow and white powders mixed together to form a greyish one. This powder was further ground in a vibrating mill and then pressed into a tablet. The tablet initially stuck to one the press pieces, but came of intact. The surfaces of the tablet were not quite as shiny as with the tablets before, but a lot sturdier. These changes might be due to an excess of MAI in the reaction. Conductivity of the disk was measured with the IV-curve measurement setup by attaching small wires with silver paint to the disk. Under illumination the tablet showed some activity while without illumination no activity was observed.

Another attempt at attaching a piece of metal to serve as an electrode was made. This time an aluminium strip was cleaned and softened by scraping and pressing with pincers. The aluminium was then wetted with 2-propanol and placed on the perovskite to see, if it would adhere itself. This was attempted with both solution processed and solid state processed perovskite. The strip stuck with neither of them, but on the surface of the solid state processed perovskite a layer of white MAI crystals formed. 2-propanol apparently frees additional MAI-ions stuck in the perovskite matrix and allows them to recrystallize on the tablet surface.

3.10 Single solution with lead iodide

A very strong solution of MAI + PbI_2 in DMF was made. The idea was to make a heated and supersaturated solution of perovskite precursors, which would then upon cooling form perovskite in suspension. Into 5 ml of DMF 50 mg of MAI and 2.305 g of PbI_2 were added. All was dissolved after thorough mixing and heating and the solution was

left to stand overnight. No precipitate formed so the amount of MAI and PbI_2 was increased in two steps first 200.5 mg and 0.1328 g and then 201.1 mg and 0.1069 g. After each step the solution was heated and stirred until the solution was clear. A glass slide was put in the solution to see if it would help crystals to form. None did however and the slide was removed and annealed at 75°C . A perovskite formed during annealing as suspected. 0.1067 g of PbI_2 was added and the solution was left to sit overnight. The solution was still clear in the morning so 0.4562 g of MAI was added to achieve a 1:1 molar ratio of MAI to PbI_2 . The weight% of the solution is now about 43%. A glass slide was put in the solution overnight to see, if any crystals would form. None did. Absorption spectra of the solution were measured, but before a clear spectrum could be measured the solution had to be diluted three times 20:300. The high absorption coefficient is due to complexes in the solution and the complexes unravel in more dilute solutions so the clear spectrum looked just like the ones measured earlier.

3.11 Suspension in 2-propanol

25 μl of the 43 m% equimolar MAI: PbI_2 solution was injected into 500 μl of pure 2-propanol. The purpose of this experiment was to see, if smaller perovskite crystals would form in this way than by sprinkling perovskite on MAI in 2-propanol. This was done as solubilities of MAI and PbI_2 are lower in 2-propanol than in DMF. A lot of white crystals formed almost filling the vessel. Some of the crystals had a yellowish tint indicating the presence of lead iodide. No black perovskite was observed however.

Another similar experiment was performed but this time the solution to which the MAI: PbI_2 solution was injected was not pure 2-propanol but 2-propanol with 10 mg/ml MAI. The excess MAI could assist in the formation of the perovskite. Once again upon injection a lot of white crystals with a greyish tint formed. The suspension was sonicated for five minutes and when the grey appeared to deepen another five minutes more. The grey deepened further and the solids came to rest on the bottom of the tube. The liquid phase appeared yellow.

Samples of both of the two injection experiments were deposited onto glass slides and then annealed at 50°C , 70°C and 100°C for ten minutes at each temperature. The slides were photographed at each stage with the Dino-Lite AM4113ZTL microscope. Already at 50°C the 2-propanol dried and perovskite started to form. At higher temperatures the reaction did appear to go further as the colour of the samples darkened. The rest of the suspension was sealed and stored in a refrigerator, but after a few days of storage all black had vanished. Maybe the 2-propanol has absorbed water from air and the water in the 2-propanol has destroyed the perovskite.

3.12 Mixed halides

0.4076 g of PbCl_2 was put into 5 ml of DMF and set to heat and stir on a hot plate at 75°C . The lead chloride failed to dissolve so 1 ml of DMF was added and the solution

was left to stir overnight. The presence of MAI assists the dissolution of lead halides as mentioned by Tidhar et al. (2014). Therefore MAI was added. It was added in three steps, first 0.2322 g, second 0.2358 g and third 0.2317 g, with heating and stirring after each addition. The amount of MAI now equaled a 3:1 molar ratio, which is the ratio required to make perovskites out of a single solution with only lead chloride as the lead source. Even at this ratio all of the solids failed to dissolve so a further 0.0600 g of MAI was added and now all seemed to dissolve. The mass% was 17%.

Two samples were spin coated onto glass slides with a compact TiO_2 layer. One slide was preheated and the other was not. The solution was heated to 70°C for both samples. The spin coater had the same parameters for both as well, 2000 rpm for 1 minute with a slow ramp (2000 rpm was achieved only after 29s). The samples were annealed in an exicator at 110°C and stored there overnight. In the morning after closer inspection the coverage in the samples was very poor and this was deemed to be because the solution was too dilute. In previous experiments preheating the slide improved coverage greatly. In this case it did as well, but still the coverage was very bad.

A stronger solution was made of one sixth of the original. The volume of the solution was 1 ml and to this MAI and PbCl_2 were added both in two sets respectively 0.1423 g and 0.0796 g and 0.1447 g and 0.0761 g. The achieved m% was 41.03% and the molar ratio of MAI to PbCl_2 3.25.

Two samples were spin coated from the stronger solution onto glass slides with a compact TiO_2 layer. This time both slides were preheated but with one of the slides after the deposition of MAI- PbCl_2 there was a three minute wait before starting the spin coater, as Aharon et al. (2014) had experimented that this gives the best results. Another sample with the same 3 min wait was prepared with a lead iodide solution from one of the older experiments. The spin coating settings were the same as before. After spin coating the slides were annealed in air at 75°C for 30 min. After 30 min the temperature was increased to 100°C . The films appeared reddish brown.

Two MAI solutions in 2-propanol were prepared in two 4 ml test tubes. Both had the concentration of 10 mg/ml. One tube was heated to 75°C and the other was kept in room temperature. Lead chloride was then sprinkled on the solutions with a tiny spoon to see if perovskite formation takes place with PbCl_2 and MAI in 2-propanol. The other tube was heated to see whether an elevated temperature would assist in perovskite formation as implied by Tidhar et al. (2014), however even in the sample at room temperature the transformation to perovskite was visibly instantaneous and no distinction could be made between elevated and room temperature. Another thing was tried with sample 2 though, a larger amount of PbCl_2 was added than could possibly be turned into perovskite. Regardless the powder that descended to the bottom of the tube was black until eventually it first took a little bit longer for the powder to turn black and then the powder only turned grey. This implies that just like with lead iodide also with lead chloride the perovskite formation only takes place on the surface of the granules and most of the lead halide remains unreacted. The following day all the powder of sample 1 re-

mained black, while in sample 2 the unreacted lead chloride had separated to the top and the powder appeared more white than black.

Experiments were made with the solubility of lead chloride in DMF. The incentive was to make a supersaturated solution of PbCl_2 . However this proved more difficult than expected. As reference solubilities the ones reported by Williams et al. (2014) were used. These solubilities can be seen in Table 3.1. With heating and stirring the reference solubilities by Williams et al. were higher than what could be dissolved in these experiments. 2 ml of DMF was taken into a 4 ml test tube and lead chloride was added in small steps with a tiny spoon. This was continued until no more would dissolve. On several occasions the following morning the supersaturated solution of the previous day had dissolved all of the lead chloride. Every time a little more was added and the solution was set to heat and stir and a white powder would remain. Finally an experiment was made with the solution that had clarified and dissolved over the weekend. The solution was set on hot plate without adding any lead chloride. After a short period of time white crystals were formed. Most of the crystals dissolved again as the solution cooled. This indicates that lead chloride is more soluble in DMF in cool temperatures. Apparently it forms some complexes with the solvent and the formation of these complexes is an exothermic reaction.

Table 3.1. Solubilities of three different lead halides in DMF. (Williams et al. 2014)

bond	D (kJ/mol)	solubility in DMF (g/mL)
Pb-Cl	243	0.08 ± 0.01
Pb-Br	201	0.17 ± 0.02
Pb-I	142	0.36 ± 0.01

A set of four solar cells were manufactured with the single solution process technique. The effects of spin speed and the ramp of that speed on cell morphology were studied. The cells were made on substrates with a 300 nm thick layer of mesoporous TiO_2 from 200 μl of DMF with 41.03 m% of lead chloride and methylammonium iodide in the ratio of 1:3. The first sample was the reference sample. The spin coating preferences for this were 2000 rpm, 1 minute and slow ramp. These were the same as for all samples thus far. For the rest of the samples a lot faster ramp was used. With these settings it only took 5-10s for the spin coater to reach its designated speed in comparison to the 27s it took with the slow ramp. Also the designated rpm was raised in increments of 2000 rpm from 2000 rpm to 6000 rpm. After the spin coating the samples were annealed at 90°C in N_2 atmosphere. Absorption and transmittance spectra were measured for all samples. Gold electrodes were evaporated on 8 samples with the mixed halide perovskite. Then

the slides were encapsulated with the same method as described earlier and their I-V curves were measured.

3.13 A set of mixed halide solar cells with 95:5 ratio of PbI_2 to $PbCl_2$

A solution of DMF with lead iodide and lead chloride was prepared. 0.1152 g of $PbCl_2$ was weighed into a 10 ml test tube followed by 2.1897 g of PbI_2 then 5 ml of DMF. The solution was set to heat and stir at 75°C overnight. In this set there were 16 substrates all of which had 600 nm of mesoporous TiO_2 . The samples were numbered 1 to 16 on the backside of the substrate. All samples were spin coated once and samples 9-16 twice with fast ramp and 2000 rpm as the previous experiment indicated this would give the best results. Other variations between the samples were the concentration of the methylammonium iodide solution in which they were dipped as well as the temperature of that solution. The specific conditions for each sample in the test can be seen in Table 3.2. After spin coating the first layer of lead halide the absorption spectra of all substrates were measured. The spectra were measured again for samples 9-16 after adding the second coating of lead halide.

Altogether four sets of methylammonium iodide in 2-propanol were made, two for each temperature, 60°C and room temperature, and two for each concentration, 10 mg/ml and 14 mg/ml. Each dipping had its own MAI-solution to make sure the concentration of MAI is the same as well as to make sure that no additional contaminants from the previous set of cells would remain. The solutions were made in two sets first 5 ml each and then another set of 25 ml so that the combined volume of each two sets was 30 ml.

The dipping was done in Gram stainers. For the samples in room temperature the MAI-solution was carefully poured on the substrates and the samples with heated MAI-solution were placed one by one in the Gram stainer with pincers. The dipping time was 15 minutes as according to Cao et al. (2014) this is the optimum dipping time. After dipping the substrates were put on a sheet of foil in an exicator set at 90°C for 42min.

Table 3.2. Experimental conditions for samples 1-16 in the 2-step deposition mixed halide experiment.

Sample#	# of coats	Dipping conditions	Sample#	# of coats	Dipping conditions
1	1	10 mg/ml room temperature	9	2	10 mg/ml room temperature
2	1	10 mg/ml room temperature	10	2	10 mg/ml room temperature
3	1	14 mg/ml room temperature	11	2	14 mg/ml room temperature

4	1	14 mg/ml room temperature	12	2	14 mg/ml room temperature
5	1	10 mg/ml 60°C	13	2	10 mg/ml 60°C
6	1	10 mg/ml 60°C	14	2	10 mg/ml 60°C
7	1	14 mg/ml 60°C	15	2	14 mg/ml 60°C
8	1	14 mg/ml 60°C	16	2	14 mg/ml 60°C

Initially the samples were very dark, especially the ones from the heated MAI-solution, but after the initial annealing white crystals formed on top of the samples. After 42 minutes of 90°C the temperature was increased to 120°C and after 180 minutes it was increased to 150°C. After 205 minutes the annealing was stopped, however the white crystals had not sublimated as suspected, and the samples were left to cool under vacuum. Once cool the samples were rinsed with 2-propanol to remove the white methylammonium chloride crystals and then heated on a hot plate at 100°C to evaporate the 2-propanol. The films turned bluish. The white crystals on the cells and the bluish colour after 2-propanol wash can be seen in Figure 3.4.



Figure 3.4. Solar cells before and after 2-propanol wash.

The edges of the substrates were cleaned with a cotton swab dipped in ethanol. To make the glass covers attach more efficiently. The samples were stored in an exicator overnight. The next day the rest of the edges were cleaned and 91.6 nm thick gold electrodes were evaporated on the substrates. Then the substrates were encapsulated. After encapsulation the I-V curves were measured. Regardless of the cleaning of the edges the covers of samples 13, 11, 9 and 5 broke off during I-V measurements and were reattached

on a hot plate by heating and applying pressure with tweezers. In light of this the encapsulation procedure is clearly not optimal and should still be improved.

4 RESULTS

This section includes all the most important results of the experiments described in section 3. Only a fraction of all the acquired spectra is displayed here as there are a lot of them. The rest of the spectra and graphs can be found in appendix 1.

4.1 Lead iodide films on glass substrates

The first set of experiments was mostly about getting to know the equipment and the workings of the laboratory. The tests done were rather simple. Still the results agree well with the expectations. The absorption, transmittance, reflectance and emission spectra of lead iodide and perovskite agree with literature data. One surprising piece of data is that applying a second spin coating of PbI_2 in DMF actually lowers the absorbance of the sample. Some spectra acquired from the samples are shown in Figure 4.1.

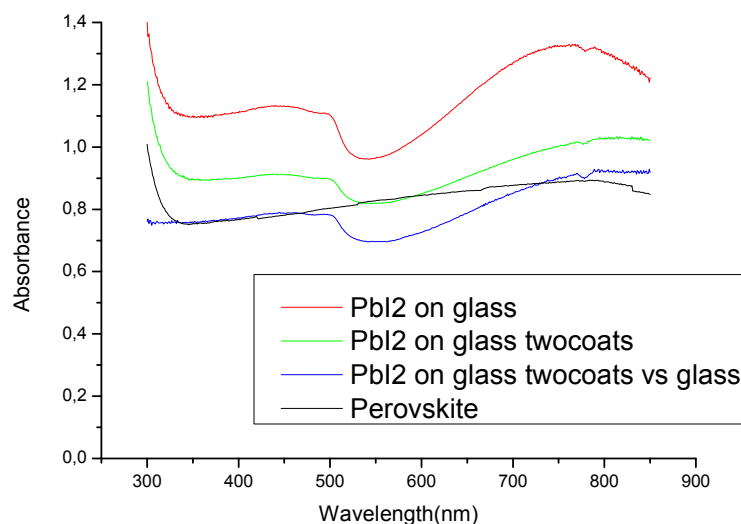


Figure 4.1. Absorption spectra of glass slide number 2, the red, green and black lines are measured with nothing in the other sample holder while for the blue line a clean glass slide was placed in it.

4.2 First solar cells with the recipe from Shi et al.

The results from the first cells were none too encouraging with the PCE of the best cell being around a meagre 1 % and six out of eight cells not even working. Regardless at least some photoactivity was achieved and it could be said that the recipe worked although rather poorly. A picture of the best working cell of this batch can be seen in Figure 4.2. This picture and all pictures with magnification in the same range were taken

with the dinolite microscope. The active area is circled in red and this area was used to calculate the current densities. The unevenness of the sample can be clearly seen even with the naked eye and is quite evident in Figure 4.2's 35.2x magnification. This lack of uniformity in the film is not desirable and harmful for the cell's performance as can be deduced from the poor performance compared to Shi et al. (2014a) and the fact that most cells short circuited. The I-V curve of the best sample can be seen in Figure 4.3.

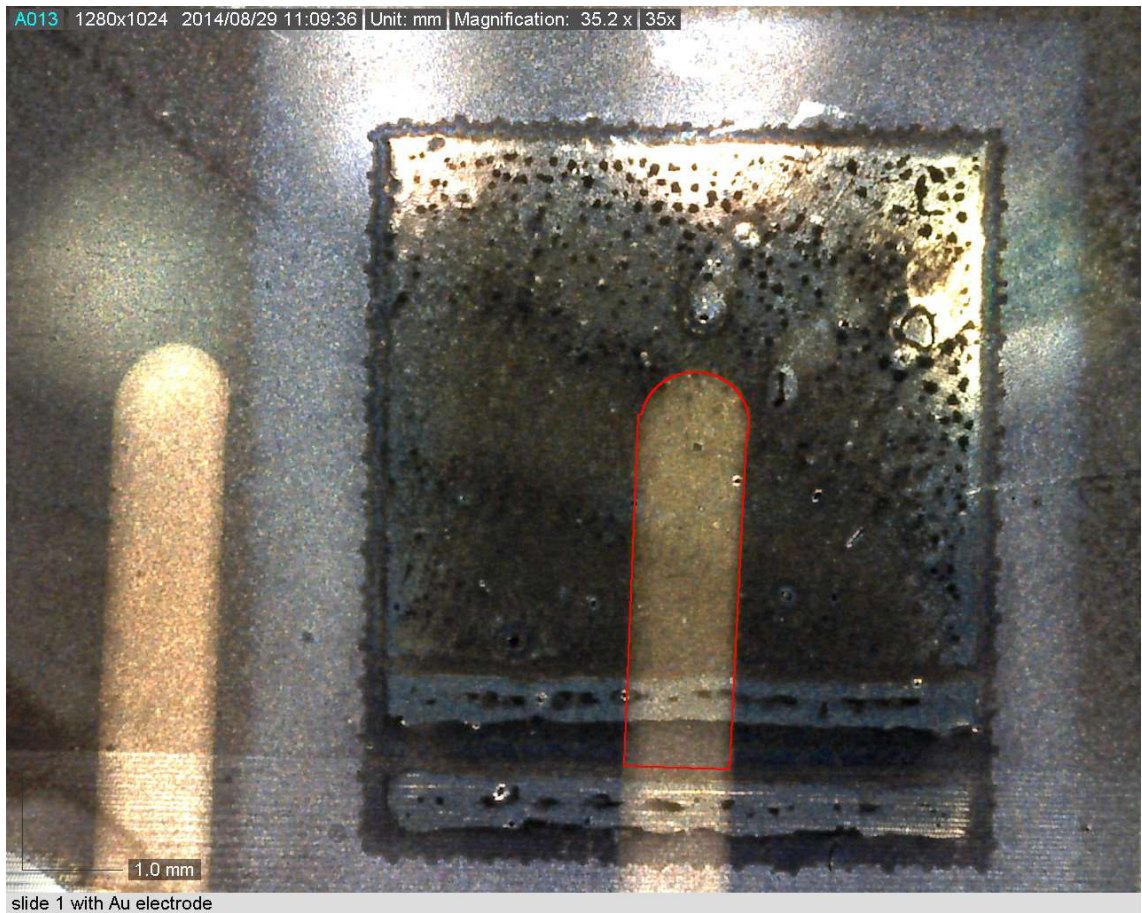


Figure 4.2. Sample number one of the first set of solar cells, the active area has been encircled with red

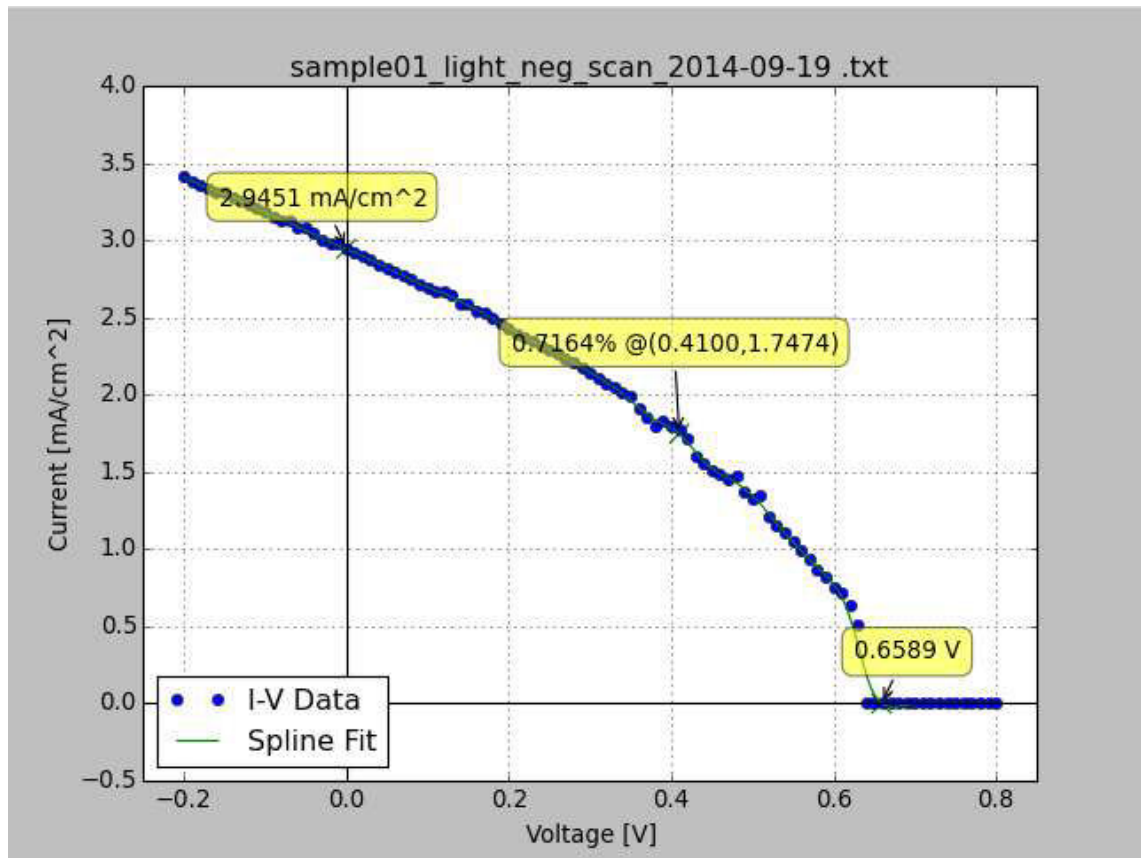


Figure 4.3. I-V curve of sample 1

4.3 Refining the process of making a uniform layer of perovskite

The lack of uniformity of the perovskite film was identified as the key factor, which caused poor performance. Therefore a set of experiments was conducted to improve film quality and thickness. The tests were performed on glass to conserve the not as readily available substrates from Solaronix. The lack of uniformity was confirmed by SEM-images of sample 7. (Figure 4.4) The titanium dioxide layer can clearly be seen in some places.

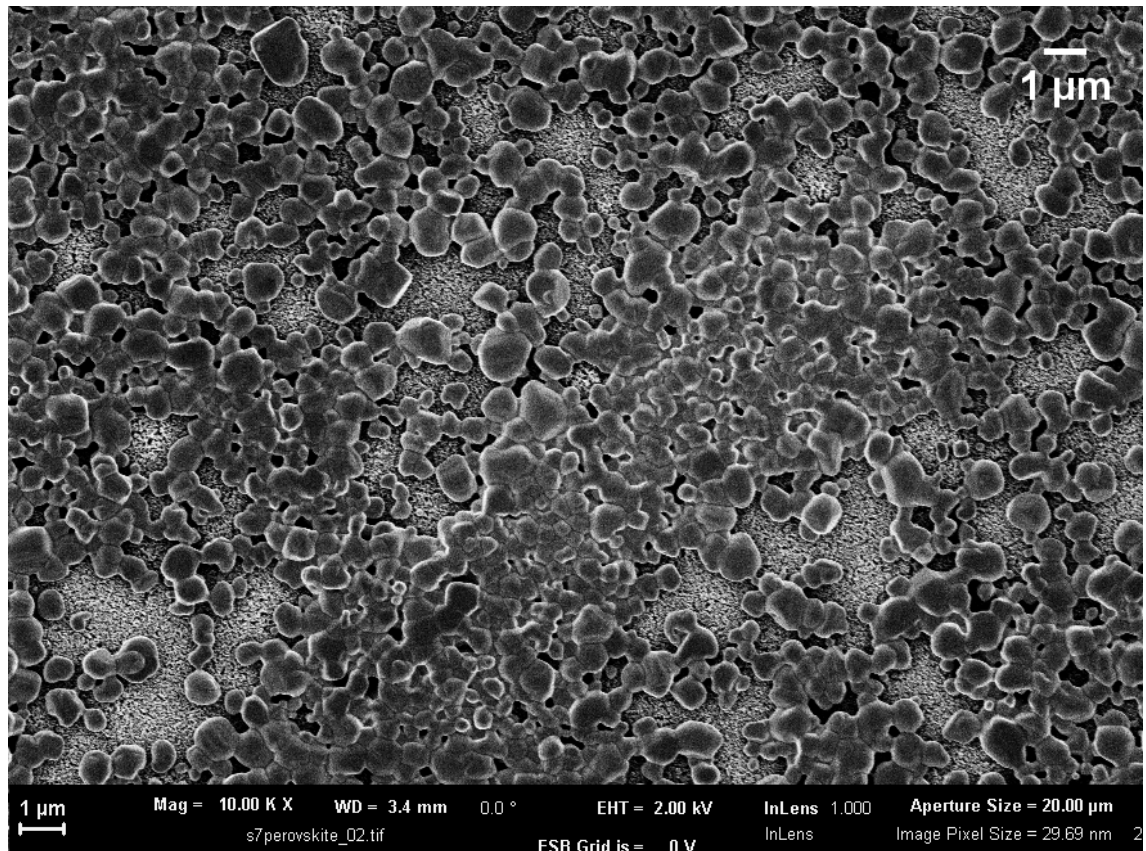


Figure 4.4. SEM-image of sample 7.

First a more dilute solution of lead iodide was prepared. The idea was that a more dilute solution would crystallize into a smoother film and three coats were applied to ensure sufficient thickness. The glass slides appeared almost colourless to the naked eye and when compared with the absorption spectra from other experiments the films acquired were very bad. After being dipped in MAI the slides had hardly any perovskite on them.

The other two experiments were performed with a stronger solution of PbI_2 . Another attempt was made to fix a solution with the concentration of 1.2 M as was reportedly used by Shi et al. Once again the highest concentration achieved was 1 M. Compared with literature values (Tidhar et al. 2014) even this 1 M was higher than what they acquired in room temperature, so the rest of the experiments with lead iodide were performed with a solution concentration of 1 M.

An experiment where the glass slides were scratched with sandpaper to see, if the lead iodide and therefore perovskite crystals as well would align with these scratches, was conducted. But microscope images of the slides showed that no such orientation happened. The crystals formed like before. Figure 4.5 shows a microscope image of one of the slides and a clear indication that crystal orientation is not dependent on scratches on the substrate surface.

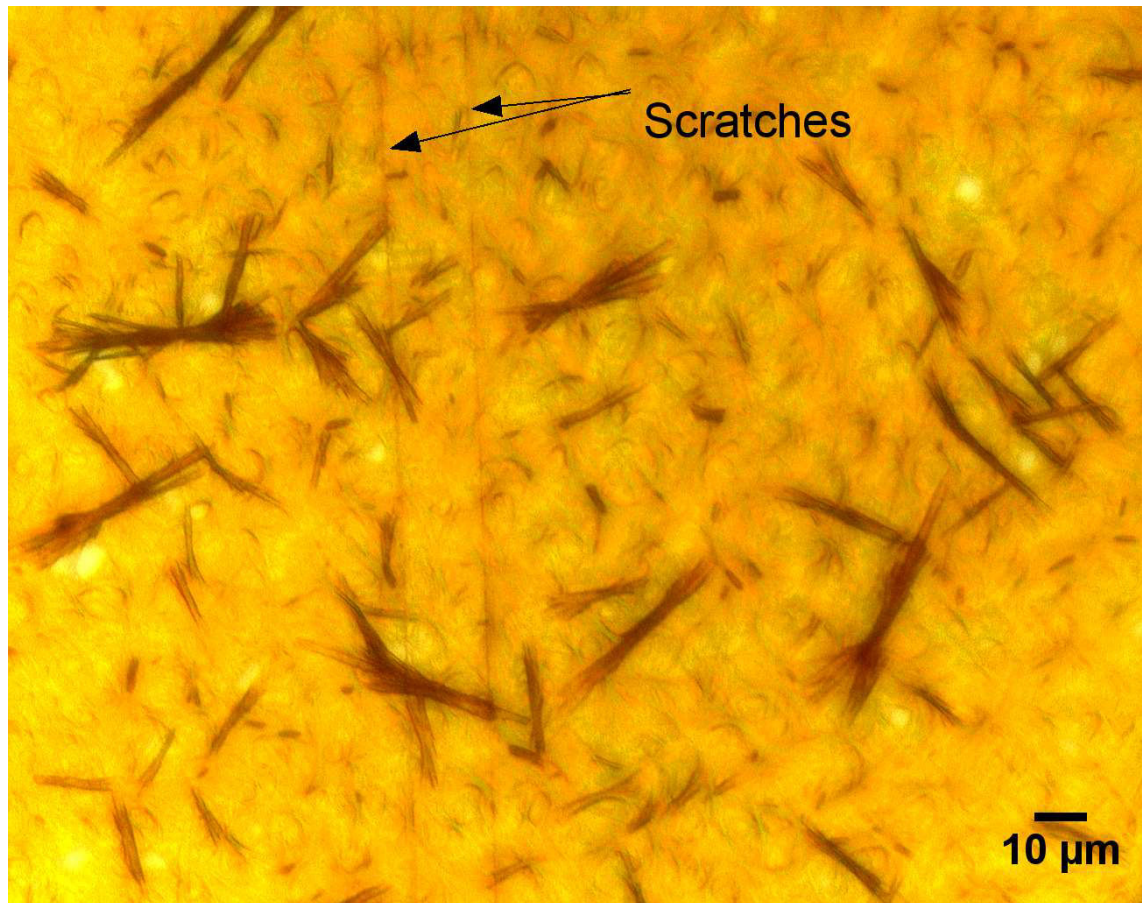


Figure 4.5. Lead iodide on scratched glass surface.

Shi et al. described their experimental process rather ambiguously and some misinterpretations were made. But apparently they heated their substrates for spin coating. This was tried and the resulting film colour was significantly more intense. Also the absorption spectra measured were more intense. Microscopic images showed better coverage as well. The heating of substrates was deemed the improvement to be made in the process for the next batch of cells.

4.4 Second set of solar cells

All the cells in the second set worked and the best cell achieved a PCE of 2.7%. This still isn't nearly as good as with the reference paper. Still the recipe modified for our laboratory produced working solar cells. This enabled the conduction of further experiments like decay over time for protected cells and the functionality of the protective glass. The efficiencies and variations in cell recipe can be seen in Table 4.1.

Table 4.1. Recipe variations and efficiencies of solar cells from the second batch.

Sample#	# of coats	Thickness of TiO ₂	Concentration of MAI-solution and dipping time	PCE% (pos./neg.)
9	2	300 nm	10mg/ml 60min	0,7/0,6
10	2	300 nm	10mg/ml 60min	2,0/1,7
11	2	300 nm	10mg/ml 120 min	1,4/1,2
12	2	300 nm	10mg/ml 120 min	2,2/2,7
13	2	600 nm	10mg/ml 60 min	1,1/1,2
14	2	600 nm	10mg/ml 60 min	1,6/1,6
15	2	600 nm	10mg/ml 120 min	1,1/1,3
16	2	600 nm	10mg/ml 120 min	1,5/1,2

The results are rather erratic so the influence of any of the varied parameters in this test is unclear. The film uniformity was still rather poor and most likely the differences in performance are explained by this. No titanium dioxide was clearly visible in the SEM-images, but there are great differences in the height of the surface. There might be cracks in the perovskite and/or the gold electrode unseen in the SEM. A SEM-image of sample 14 is shown in Figure 4.6. The actual cell is only a fraction of the perovskite film and when the inconsistencies can be seen with the naked eye, the position of the gold electrode has a huge role in cell performance.

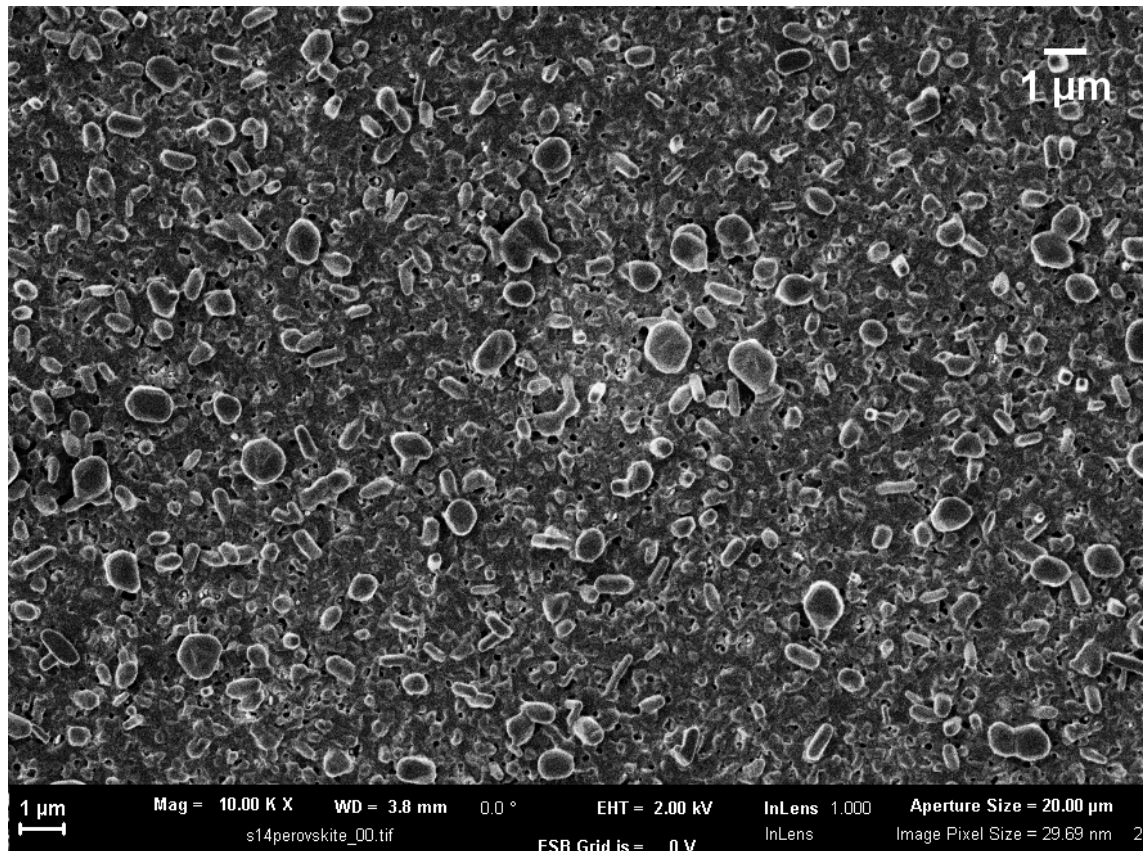


Figure 4.6. SEM-image of sample 14.

4.5 Monitoring the decay of the solar cells and further experiments with the solar simulator

As all the cells in the second batch worked, more extensive measurements were carried out. These measurements showed that the best efficiencies were always acquired from the first set of scans. When measured immediately after the first scan the second scan gives worse results and this continues at least up to 5 consecutive scans. A short period in the dark recovers the samples somewhat and a longer period of darkness allows them to return to almost original efficiency. Apparently some kind of photoactivated reorganization of ions happens in the perovskite affecting the photoactive properties of the material. (Unger et al. 2014)

The effect of constant voltage under illumination on solar cell efficiency is clearly detrimental. Sample 10, which was used for these experiments, weakened significantly. It went from about 2% PCE to that of less than 0.5%. Also during the measurements the observed current never stabilised. For the entire 60 minute measurement period the photocurrent through the cell decreased. In the experiment where the measurement time was increased to 100 min something went wrong and the results showed the exact opposite, that the current would be decreasing, but it didn't stabilise in this case either.

The I-V curves of cells labelled 1 and 9-16 were measured at approximately one week intervals for a period 31 days. The lines show a slight decrease in functionality as a function of time. Figure 4.6 shows the curves for sample 11.

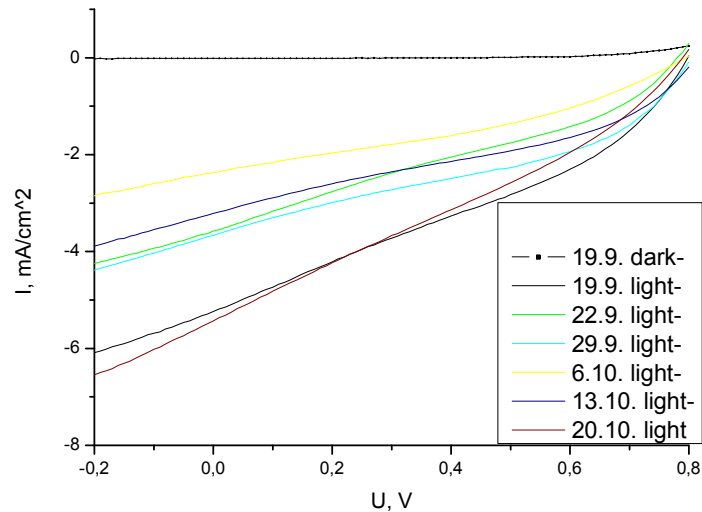


Figure 4.6. I-V curves of sample 11 over the course of 31 days.

4.6 Durability test

The durability test was done to see how well the protective cover works in comparison to unprotected samples. The test was very similar to the one conducted by Habisreutinger et al. (2014). In Figures 4.8 to 4.11 the progress of the test can be seen. After 24 h the uncovered cells already start to convert back to lead iodide, after 48 h there is almost no perovskite left and after 87 h there is no visible perovskite left. On the other hand in the protected sample almost no perovskite converts to lead iodide. The test and the fact that all other protected cells have endured visibly well indicates that the protective cover shields the samples well against ambient air.

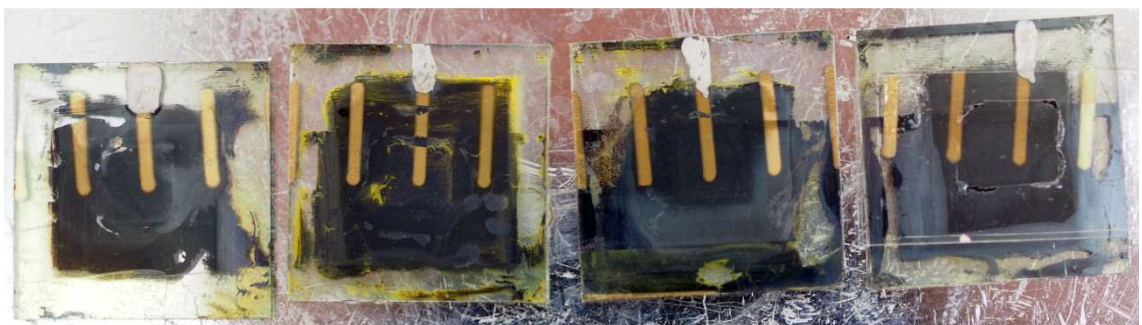


Figure 4.8. Samples 13 0 h, 14 24 h, 15 24 h (0 h uncovered), 16 0 h.

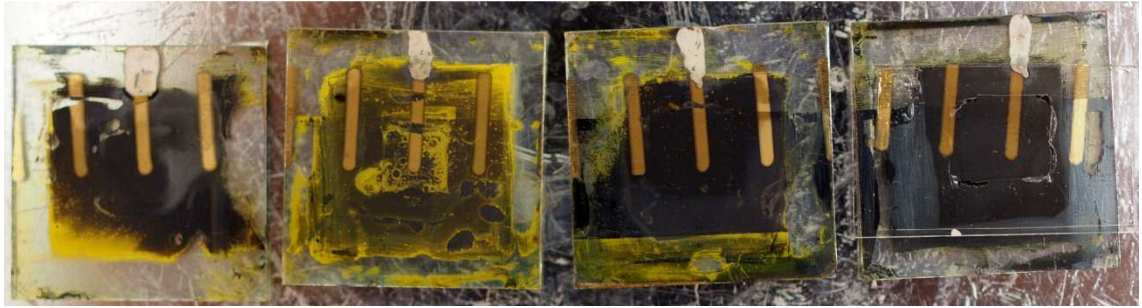


Figure 4.9. Samples 13 17.5 h, 14 41.5 h, 15 41.5 h (17.5 h uncovered), 16 17.5 h.



Figure 4.10. Samples 13 24 h, 14 48 h, 15 48 h (24 h uncovered), 16 24 h.

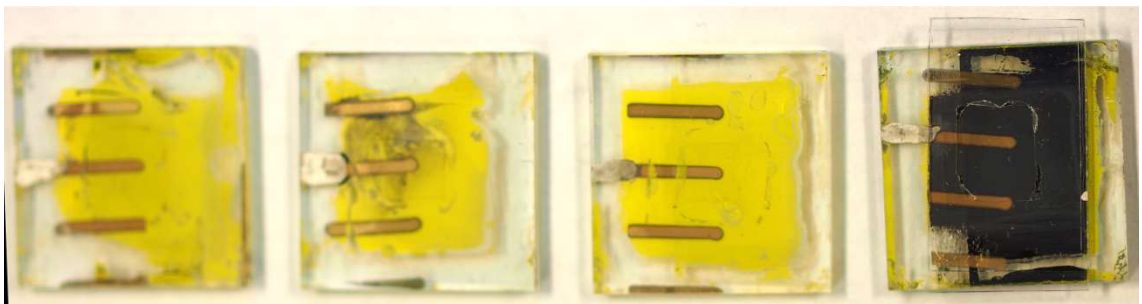


Figure 4.11. Samples 13 87 h, 14 111 h, 15 111 h (87 h uncovered), 16 87 h.

4.7 Perovskite pellets by pressing from powder

The experiments were performed to see whether it would be feasible to separate the perovskite formation from the film making and thus open new ways to manufacture perovskite cells via for example roll to roll compressing. These experiments showed among other things that perovskite forms only on the surface of lead iodide. Even when ground into a very fine powder most of the methylammonium iodide in 2-propanol unreacted as seen from Figure 4.12, which shows the absorption spectra measured from the MAI-solution used for making perovskite powder after the lead iodide was added. Furthermore the absorption seems to intensify as time goes on. This could be due to the still high concentration and possible aggregation. This might be caused by some kind of a complex formation in the solution. The same reaction may be the cause for the colour change from colourless to yellow in freshly made methylammonium iodide solutions.

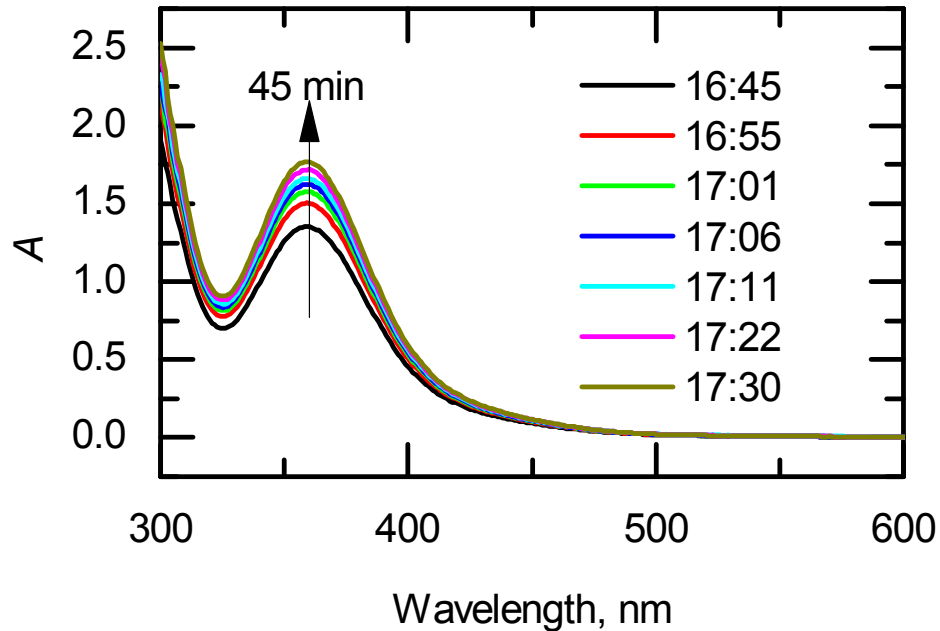


Figure 4.12. Absorption spectrum of MAI-solution after perovskite reaction.

Experiments also showed that perovskite forms a sludge that sticks effectively to most surfaces in the laboratory. Perovskite is compressible and the acquired tablets are very brittle and hard to remove from the press intact and to handle. The tablets have a metallic sheen, which implies that they might work as semiconductors. The conductivity measurements performed on the compressed tablets showed that it had resistance in the order of magnitude of megaohms and that this resistance is lowered when the perovskite is placed under illumination. Figure 4.13 shows a perovskite tablet that has cracked as all of them did. Depending on illumination either the surface of the pellet or the insides seen in the crack have a metallic sheen while the other is not shiny.

The absorbance and fluorescence spectra were slightly different to others measured from other perovskites. The absorbance covered a wider span of the spectrum and the fluorescence had shifted to a shorter wavelength.

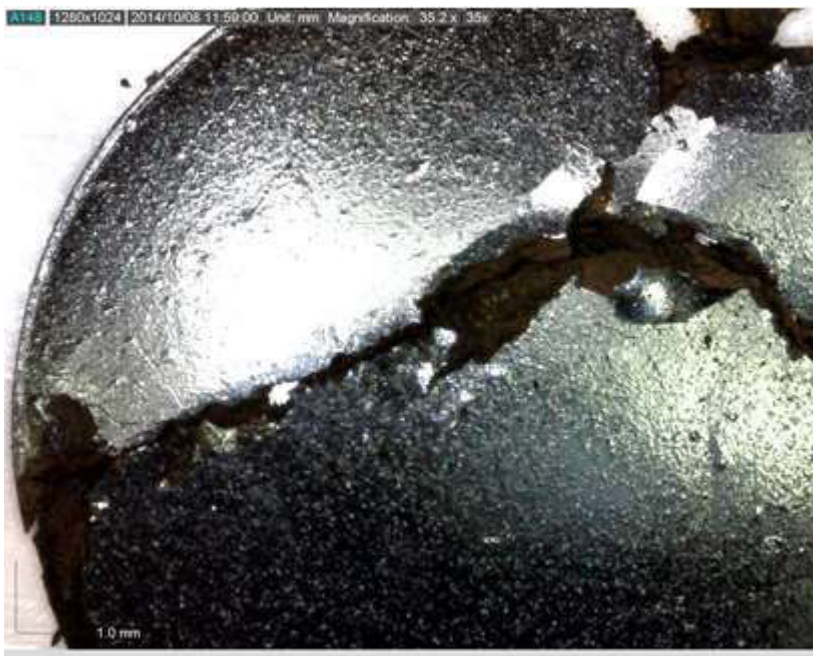


Figure 4.13. A tablet compressed from perovskite powder.

The idea of a solar cell from solid perovskite by pressing is an interesting one and given more time and effort could lead to new findings and applications. The timeframe and resources allocated for this work were too short for this, however. This method might work, if small enough perovskite crystals could be formed, so that the amount of unreacted lead iodide would be low enough. Alternatively, if via some method it would be possible to compress a thin enough layer of perovskite directly onto a substrate. This layer would need to be thinner than $1\ \mu\text{m}$, otherwise it would be too thick for the cell to function properly.

4.8 Single solution with lead iodide

The solution had 43 m% of MAI and lead iodide in a 1:1 molar ratio and it appeared rather viscous. We were unable to get perovskite to form in DMF. Maybe the amount of MAI or PbI_2 was insufficient or the complexes formed with DMF prevent the formation or then the formation requires a trigger from ambient air or then the water content of DMF was enough to keep the perovskite from forming. The glass slide deposited in the solution also didn't trigger the reaction. However when the glass slide was removed from the solution a thick layer of the solution was stuck to the slide. After drying the slide on a foil on a hot plate the perovskite formed. The formed patterns were very inconsistent as seen in Figure 4.14. The formation is not complete as the molar amount of lead iodide is greater than that of methylammonium iodide. The incomplete transformation is shown in the microscope image taken with the Zeiss Axioskop in Figure 4.15.



Figure 4.14. Perovskite from 2:1 PbI₂: MAI solution.

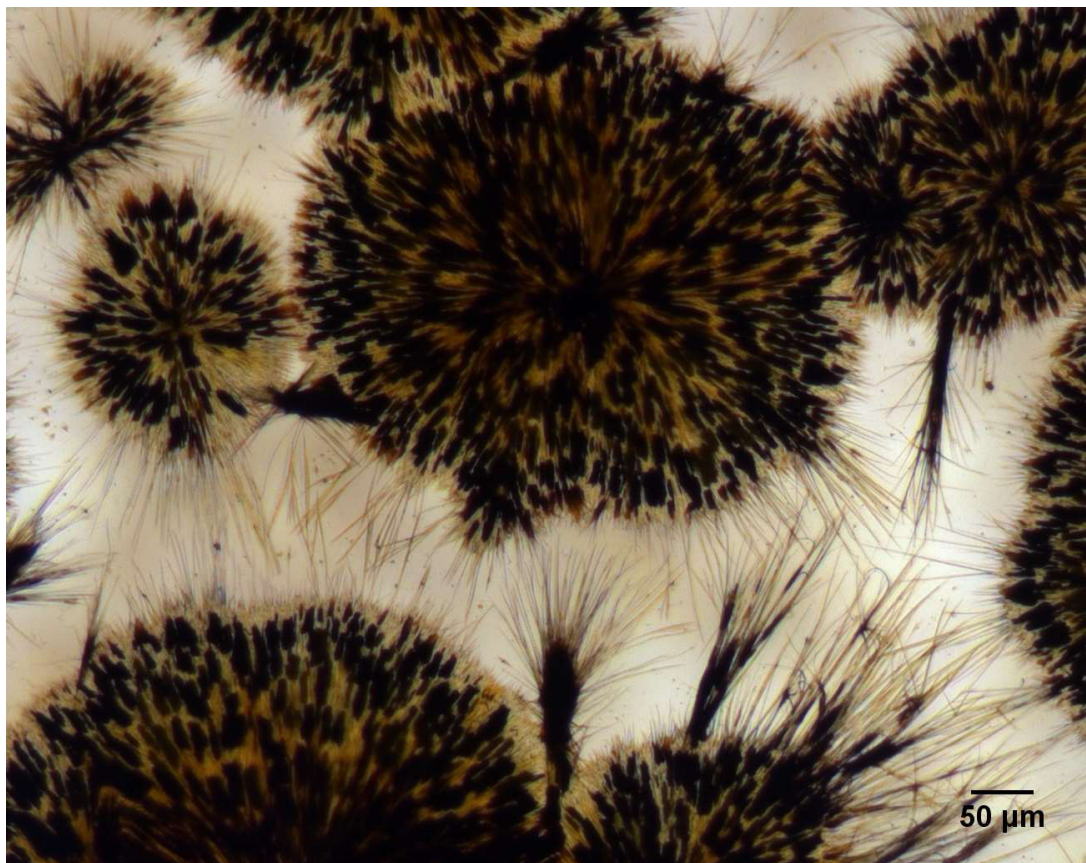


Figure 4.15. The incomplete formation of perovskite from 2:1 PbI₂: MAI solution.

4.9 Suspension in 2-propanol

As the same 43 mass-% 1:1 MAI:PbI₂ solution as used in the previous experiment was injected into 2-propanol, the formation of perovskite was instantaneous. Therefore the fact that no perovskite crystals formed in the strong single solution of its components implies, that it is DMF and the complexes it forms with the components in the solution that hinders the perovskite formation. These tests confirmed that sonication aids in making finer perovskite crystals that have less unreacted lead iodide. Also the presence of excess MAI helps in making smaller crystals. It would also seem so that perovskite is eventually destroyed in 2-propanol even though it is supposedly insoluble in it. The reason might be water that has mixed with the 2-propanol or that the methylammonium somehow loosens itself from the perovskite structure into the 2-propanol. The latter explanation is supported by the fact that the 2-propanol turns yellow when perovskite is stored in it and the solution spectrum is identical to that of methylammonium in 2-propanol.

4.10 Mixed halides

When preparing the single solution with lead chloride and methylammonium iodide it became apparent that methylammonium iodide facilitates the dissolution of lead chloride significantly. From the solutions prepared solar cells were made. Three of the cells were made on substrates with no mesoporous TiO₂ and these cells showed only negligible activity. The four cells that were made on 300 nm of TiO₂ had the experimental variations and efficiencies depicted in Table 4.2. The table also shows the maximum power points, the short circuit currents, the open circuit voltages and the fill factors for each separate scan performed.

Table 4.2. *I-V data for the mixed halide single solution solar cells.*

#sample	Spin coating conditions	PCE [%]	J_{sc} [mA/cm ²]	V_{oc} [mV]	FF (%)
s4_pos	2000 rpm slow ramp	3.6	15.1	670	35.3
s4_neg	2000 rpm slow ramp	3.8	14.1	689	38.9
s5_pos	2000 rpm fast ramp	4.4	18.9	694	33.5
s5_neg	2000 rpm slow ramp	3.0	13.6	682	32.4
s6_pos	4000 rpm slow ramp	4.0	16.4	721	33.6
s6_neg	4000 rpm slow ramp	2.5	11.1	698	32.5
s7_pos	6000 rpm slow ramp	3.4	14.3	712	33.8
s7_neg	6000 rpm slow ramp	2.4	10.1	698	34.7

The results would seem to confirm the results acquired by Etgar et al. (2014). They of course make no mention of how quickly their spin coater achieved the desired rotation speed of 2000 rpm, but in this experiment the highest efficiency was achieved with a fast ramping speed, so it seems to be more favourable than the slow ramp used until this point. This test was used and the following solar cells were spin coated using the rotation speed of 2000 rpm and a faster ramp.

4.11 A set of mixed halide solar cells with 95:5 ratio of PbI_2 to PbCl_2

These cells were the last ones made for this work and they yielded the best results as well. It is encouraging that with each iteration significant progress was made. The efficiencies of the cells made are listed in Table 4.3. Like with previous batches the variations between even cells with exactly same recipes are very much notable, so much so that it is impossible to say, if any of the variations in the recipes were favourable or not.

Table 4.3. Efficiencies of the final batch of solar cells.

Sample#	PCE% (pos. /neg.)	PCE% on 26.11.	Sample#	PCE% (pos. /neg.)	PCE% on 26.11.
1	2.5/1.7	4.4/2.7	9	4.6/3.5	5.5/4.5
2	3.1/2.4	5.2/3.6	10	1.6/1.4 , 5.5/4.3	6.3/4.5
3	0.8/0.8 , 3.9/3.2	5.2/4.2	11	0.4/0.2 , 3.0/2.7	5.2/4.2
4	6.0/4.9	6.8/5.3	12	5.3/4.6	7.2/6.0
5	1.3/0.7	7.9/4.5 , 6.9/4.9	13	7.0/5.7	5.0/3.1
6	3.6/2.6	4.0/2.6	14	7.9/4.7	5.6/3.1
7	1.6/1.7	2.4/2.1	15	Short circuit	1.2/0.8
8	4.0/2.8	5.1/3.3	16	2.8/3.3	3.7/3.8

A curious discovery was made that most of the cells had improved in efficiency when they were measured again after a few days. Partially this might be explained by the measurement conditions. The cells might have been better aligned to the light on the later day, but the fact that one of the weakest performing cells was one of the best performing cells a few days later cannot be explained by that. One possible explanation is that cells actually mature with time and the ions in perovskite are allowed to change position and this time for most of the cells the ion wandering was favourable.

5 CONCLUSIONS

In this work several basic aspects of perovskite solar cells were studied. This basic study needed to be done as the topic was new to the researchers and the research group. With this basic study a lot of basic level discoveries were made. Through trial and error, many ways, which were not ideal for making perovskite solar cells, were found. In the end the best performing solar cell made had a PCE of 7.9%. This cell was made via the sequential deposition method. This method seems to be more effective than the one-step precursor deposition method, which was the only other method tried. The cell had a mixture of lead iodide and lead chloride instead of only one of the halides. This mixture seems to be beneficial as well. The substrate of the cell was heated prior to spin coating and this definitely improves the film coverage as all samples without heating had significantly poorer coverage. In Figure 5.1 the maximum power conversion efficiencies for each cell have been documented. 1st and 2nd batch had 8 cells, while 3rd batch had only four and the 4th had 16 cells.

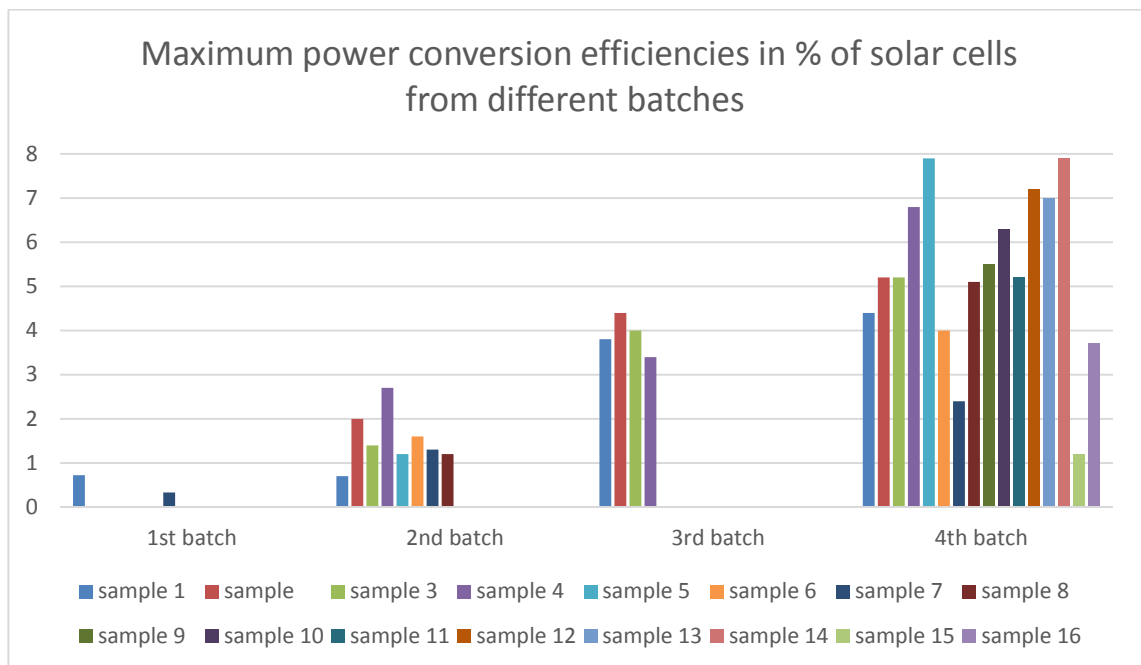


Figure 5.1. Maximum power conversion efficiencies of cells by batch.

It is hard to acquire uniform results. The results acquired were often seemingly random and it was hard to identify which settings were the best. Regardless, with every batch of cells the overall performance improved. This improvement was mostly due to further studying of the literature. Because of the seemingly random results it was difficult to deduce, which, if any, parameters were the best for cell making. Most of the improvements to the recipe found in the literature were published while we were working. This

goes to show that the field is constantly and rapidly advancing. All the time papers are being published each with more and more information on how to improve the cells.

The research topic is very hot in the world of solar cell research at the moment and it is important to make contributions to that. Further research in this work could and should be done. The work for this thesis created a basic understanding of how perovskite solar cells can be made at the Tampere University of Technology chemistry laboratory. It is easy to broaden the understanding by building on this work. A possible direction for the following research could be co-operation with the synthesis group to see how substances, for example HTMs, created at the lab would improve the perovskite cell performance. Another possibility could be the tablets pressed from perovskite powder. Looking into substrates that could have a layer of perovskite compressed on them and experimenting with the roll-to-roll manufacturing, might prove fruitful. An obvious choice for further study is of course studying how to improve the uniformity of the cells. Literature sources often report high reproducibility of cell performance, but in this work the variations between similar recipes were profound. Finding out what was done wrong would be of interest.

REFERENCES

- Aarhus University. 2013 Life deep within oceanic crust sustained by energy from interior of Earth. ScienceDaily. Available (Accessed on January 29, 2015): www.sciencedaily.com/releases/2013/03/130314144340.htm
- Aharon, Sigalit, Shany Gamliel, Bat El Cohen, and Lioz Etgar. 2014. “Depletion Region Effect of Highly Efficient Hole Conductor Free $\text{CH}_3\text{NH}_3\text{PbI}_3$ Perovskite Solar Cells.” *Phys. Chem. Chem. Phys.* 16 (22). 10512–18. doi:10.1039/c4cp00460d.
- Benanti, Travis L, and D Venkataraman. 2006. “Organic Solar Cells: An Overview Focusing on Active Layer Morphology.” *Photosynth. Res.* 87 (1). 73–81. doi:10.1007/s11120-005-6397-9.
- Burschka, Julian, Norman Pellet, Soo-Jin Moon, Robin Humphry-Baker, Peng Gao, Mohammad K Nazeeruddin, and Michael Grätzel. 2013. “Sequential Deposition as a Route to High-performance Perovskite-sensitized Solar Cells.” *Nature* 499 (7458). 316–19. doi:10.1038/nature12340.
- Cao, Duyen H., Constantinos C. Stoumpos, Christos D. Malliakas, Michael J. Katz, Omar K. Farha, Joseph T. Hupp, and Mercouri G. Kanatzidis. 2014. “Remnant PbI_2 , an Unforeseen Necessity in High-efficiency Hybrid Perovskite-based Solar Cells?” *APL Mat.* 2 (9). 091101 doi:10.1063/1.4895038.
- Coropceanu, V., Cornil, J., da Silva Filho, D. A., Olivier, Y., Silbey, R., & Brédas, J.-L. (2007). “Charge transport in organic semiconductors.” *Chem. Rev.* 107 (4). 926–52. doi:10.1021/cr050140x
- Gao, Peng, Michael Grätzel, and Mohammad K. Nazeeruddin. 2014. “Organohalide Lead Perovskites for Photovoltaic Applications.” *Energ. & Envir. Sc.* 1 (c). 2448–63. <http://xlink.rsc.org/?DOI=c4ee00942h>.
- Graph used to illustrate band filling in Wikipedia article about valence band. Available (Accessed on 16.12.2014): http://en.wikipedia.org/wiki/File:Band_filling_diagram.svg
- Green, Martin A., Anita Ho-Baillie, and Henry J. Snaith. 2014. “The Emergence of Perovskite Solar Cells.” *Nat. Photonics* 8 (7). 506–14. doi:10.1038/nphoton.2014.134.
- Green, M. A., Emery, K., Hishikawa, Y., Warta, W. & Dunlop, E. D. 2015. “Solar cell efficiency tables (Version 45)”. *Prog. Photovoltaics Res. Appl.* **23**, 1–9
- Gueymard, C.A., D. Myers, and K. Emery. 2002. “Proposed Reference Irradiance Spectra for Solar Energy Systems Testing.” *Sol. Energ.* 73 (6). 443–67. doi:10.1016/S0038-092X(03)00005-7.
- Habisreutinger, Severin N, Tomas Leijtens, Giles E Eperon, Samuel David Stranks, Robin J Nicholas, and Henry J Snaith. 2014. “Carbon Nanotube/polymer

- Composite as a Highly Stable Charge Collection Layer in Perovskite Solar Cells.” *Nano Lett.* 14 (10). 5561–68. doi:10.1021/nl501982b.
- Hoffmann, Philip. “Solid State Physics: An introduction.” Wiley-VCH, Berlin, Germany 2008 224 p. 86, 102, 103, 114 pp.
- Juarez-Perez, Emilio J, Rafael S Sanchez, Laura Badia, Germá Garcia-Belmonte, Yong Soo Kang, Ivan Mora-Sero, and Juan Bisquert. 2014. “Photoinduced Giant Dielectric Constant in Lead Halide Perovskite Solar Cells.” *J. Phys. Chem. Lett.* 5 (13). 2390–94. <http://dx.doi.org/10.1021/jz5011169>.
- Kojima, Akihiro, Kenjiro Teshima, Yasuo Shirai, and Tsutomu Miyasaka. 2009. “Organometal Halide Perovskites as Visible-light Sensitizers for Photovoltaic Cells.” *JACS* 131 (17). 6050–51. doi:10.1021/ja809598r.
- Kumar, Pankaj, and Suresh Chand. 2012. “Recent Progress and Future Aspects of Organic Solar Cells.” *Prog. Photovolt. Res. and Appl.* 20 (4). 377–415. doi:10.1002/pip.1141.
- Liu, Mingzhen, Michael B Johnston, and Henry J Snaith. 2013. “Efficient Planar Heterojunction Perovskite Solar Cells by Vapour Deposition.” *Nat.* 501 (7467). 395–98. doi:10.1038/nature12509.
- Lotsch, Bettina V. 2014. “New Light on an Old Story: Perovskites Go Solar.” *Angew. Chem. Int. Ed.* 53 (3). 635–37. doi:10.1002/anie.201309368.
- Noel, Nakita K., Samuel D. Stranks, Antonio Abate, Christian Wehrenfennig, Simone Guarnera, Amir-Abbas Haghighirad, Aditya Sadhanala, Giles E. Eperon, Sandeep K. Pathak, Michael B. Johnston, Annamaria Petrozza, Laura M. Herz and Henry J. Snaith. (2014). “Lead-Free Organic-Inorganic Tin Halide Perovskites for Photovoltaic Applications.” *Energ. Envir. Sc.* 7(9). 3061–3068. doi:10.1039/c4ee01076k
- Ponseca, Carlito S, Tom J Savenije, Mohamed Abdellah, Kaibo Zheng, Arkady Yartsev, Tobias Pascher, Tobias Harlang, Pavel Chabera, Tonu Pullerits, Andrey Stepanov, Jean-Pierre Wolf and Villy Sundström. 2014. “Organometal Halide Perovskite Solar Cell Materials Rationalized: Ultrafast Charge Generation, High and Microsecond-long Balanced Mobilities, and Slow Recombination.” *JACS* 136 (14). 5189–92. doi:10.1021/ja412583t.
- Schindelin, J., Arganda-Carreras, I., Frise, E., Kaynig, V., Longair, M., Pietzsch, T., ... Cardona, A. (2012). Fiji: an open-source platform for biological-image analysis. *Nat. Methods* 9(7). 676–82. doi:10.1038/nmeth.2019
- Service, Robert F. 2013. “Turning up the Light.” *Science (New York, N.Y.)* 342 (6160). 794–95, 797. doi:10.1126/science.342.6160.794.
- Shi, Jiangjian, Juan Dong, Songtao Lv, Yuzhuan Xu, Lifeng Zhu, Junyan Xiao, Xin Xu, Huijue Wu, Dongmei Li, Yanhong Luo, and Qingbo Meng. 2014a. “Hole-conductor-free Perovskite Organic Lead Iodide Heterojunction Thin-film Solar

Cells: High Efficiency and Junction Property.” *Appl. Phys. Lett.* 104 (6). 063901/1–063901/4. doi:10.1063/1.4864638.

Shi, Jiangjian, Yanhong Luo, Huiyun Wei, Jianheng Luo, Juan Dong, Songtao Lv, Junyan Xiao, Yuzhuan Xu, Lifeng Zhu, Xin Xu, Huijue Wu, Dongmei Li, and Qingbo Meng. 2014b. “Modified Two-step Deposition Method for High-efficiency TiO₂/CH₃NH₃PbI₃ Heterojunction Solar Cells.” *ACS Appl. Mat. Interf.* 6 (12). 9711–18. doi:10.1021/am502131t.

Snaith, Henry J. 2013. “Perovskites: The Emergence of a New Era for Low-Cost, High-Efficiency Solar Cells.” *J. Phys. Chem. Lett.* 4 (21). 3623–30. doi:10.1021/jz4020162.

Solaronix products and materials catalogue, Solaronix, website. Available (accessed on 16.12.2014): http://www.solaronix.com/documents/solaronix_materials.pdf

Tidhar, Yaron, Eran Edri, Haim Weissman, Dorin Zohar, Gary Hodes, David Cahen, Boris Rybtchinski, and Saar Kirmayer. 2014. “Crystallization of Methyl Ammonium Lead Halide Perovskites: Implications for Photovoltaic Applications.” *JACS* 136 (38). 13249–13256. doi:10.1021/ja505556s.

Unger, Eva Lisa, Eric T Hoke, Colin D Bailie, William H Nguyen, Andrea Ruth Bowring, Thomas Heumuller, Mark Greyson Christoforo, and Michael D. McGehee. 2014. “Hysteresis and Transient Behavior in Current-voltage Measurements of Hybrid-perovskite Absorber Solar Cells.” *Energ. Envir. Sc.* 7 (11). 3690–98. doi:10.1039/C4EE02465F.

Van Zeghbroeck, Bart. 2011. “Principles of Semiconductor Devices.” Available (accessed on 29.12.2014): http://ecee.colorado.edu/~bart/book/book/chapter2/ch2_7.htm

Williams, Spencer T, Fan Zuo, Chu-Chen Chueh, Chien-Yi Liao, Po-Wei Liang, and Alex K. -Y. Jen. 2014. “Role of Chloride in the Morphological Evolution of Organo-Lead Halide Perovskite Thin-Films.” *ACS Nano* October. doi:10.1021/nn5041922.

Xing, Guichuan, Nripan Mathews, Shuangyong Sun, Swee Sien Lim, Yeng Ming Lam, Michael Grätzel, Subodh Mhaisalkar, and Tze Chien Sum. 2013. “Long-range Balanced Electron- and Hole-transport Lengths in Organic-inorganic CH₃NH₃PbI₃.” *Science (New York, N.Y.)* 342 (6156). 344–47. doi:10.1126/science.1243167.

Yin, Wan-Jian, Yanfa Yan, and Su-Huai Wei. 2014. “Anomalous Alloy Properties in Mixed Halide Perovskites.” *J. of Phys. Chem. Lett.* October. 3625–31. doi:10.1021/jz501896w.

Zhou, Huaxing, Liqiang Yang, and Wei You. 2012. “Rational Design of High Performance Conjugated Polymers for Organic Solar Cells.” *Macromol.* 45 (2). 607–32. doi:10.1021/ma201648t.